
Transesophageal Three-Dimensional Echocardiography in Congenital Heart Disease

Gerald Ross Marx

Abstract

In the past 10 years, real-time three-dimensional echocardiography has emerged as an important new technique in echocardiography for the diagnosis and evaluation of both acquired and congenital heart disease. In recent years, three-dimensional transesophageal echocardiography (3D TEE) probes have become available. While these probes were designed primarily for use in the adult age group, they have also been utilized effectively in older children and adolescents. These probes are capable of real-time 3D TEE imaging and color flow Doppler, providing excellent spatial detail of selected acquired and congenital heart defects. Thus 3D TEE serves an important and ever-increasing role during cardiac surgery as well as interventional cardiology procedures. This chapter describes the technique of 3D TEE imaging as well as some of its most common applications for congenital heart disease evaluation.

Keywords

Transesophageal echocardiography • Three-dimensional echocardiography • Atrial septal defect • Subaortic stenosis • Atrial septal defects, transcatheter closure • Ebstein anomaly of the tricuspid valve

History and Development

With the advent of matrix array transducers and sophisticated computer analysis, three-dimensional (3D) echocardiography is now widely applied in the diagnostic imaging domain for congenital heart disease (CHD). In particular, congenital heart surgeons, in the operative management of complex CHD, will sometimes request 3D imaging to provide additional information about cardiac anatomy and spatial relationships. This also applies for repair of valve dysfunction, in which the anatomic substrate can be difficult to discern with standard two-dimensional (2D) imaging.

In the initial development of 3D echocardiography, a reconstructive approach was first utilized. This consisted of sequential acquisition of multiple transesophageal 2D

echocardiographic images, followed by offline reconstruction and 3D rendering of the collected image dataset [1–6]. During image acquisition, the probe was moved in a linear or rotational format, and was advanced to subsequent imaging planes, based on electrocardiographic (ECG) and respiratory gating. Excellent 3D gray scale and color flow studies were obtained. However, this technology was time consuming and cumbersome. Depending on the heart rate, the acquisition would last at least 3–5 min. Significant arrhythmias would interfere with the acquisition. Moreover, to maintain spatial integrity, the heart had to be stationary from a positional standpoint. Furthermore, the formatting of the 2D images into a 3D construct consumed additional valuable time. Although certain dedicated and cooperative surgeons would participate, this form of 3D imaging was not widely applied in the operative suite.

G.R. Marx, MD
Department of Cardiology, Boston Children's Hospital, Harvard School of Medicine, 300 Longwood Ave., Boston, MA 02115, USA
e-mail: gerald.marx@cardio.chboston.org

The online version of this chapter (doi:[10.1007/978-1-84800-064-3_19](https://doi.org/10.1007/978-1-84800-064-3_19)) contains supplementary material, which is available to authorized users.

With advancements in probe design, and sophisticated, efficient and fast computers, nearly simultaneous imaging of volumetric echocardiographic 3D data sets became available for transthoracic echocardiography transducers. These advanced matrix array transducers were relatively smaller. Hence, epicardial 3D echocardiography evolved as these matrix array probes could be held and manipulated comfortably on the heart by the surgeon [7]. The surgeon could investigate the anatomy in the “live” 3D display. Similar to 2D imaging, immediate anatomic “feedback” was available, but in a 3D spatial orientation. Even full volume acquisitions could be obtained, and the specific anatomy segmented and displayed to the surgeon in minutes.

Although excellent 3D images could be shown in the operating room, available for surgical planning, certain disadvantages with epicardial 3D echocardiography were apparent. First, imaging in the near field was sub-optimal due to the very short focal distance. Second, in the vigorously beating heart, stable contact of the transducer with the cardiac structures was difficult to maintain. Third, this type of image acquisition occupied and usurped the time and concentration of the operating surgeon [8]. These important limitations, coupled with the development of a real-time 3D transesophageal echocardiography (TEE) probe in 2007 (X7-2t, Philips Medical Systems, Andover, Massachusetts) [9], have led to the use of 3D TEE as the preferred 3D technique in the operative setting (for patients of adequate size). Despite this important achievement, epicardial 3D echocardiography can still be used: (1) for young and small pediatric patients in whom the 3D TEE probe is too large; (2) for those pediatric or adult patients with specific contraindications to TEE.

3D TEE has readily become accepted for adult patients undergoing cardiothoracic surgery or catheter-based interventions [9–12]. This technological advancement has also been applied to adult patients with congenital heart defects. However, with careful patient selection, and collaboration between the cardiologist and anesthesiologist, 3D TEE can be used safely in selected children and adolescents [13]. As opposed to epicardial imaging, 3D TEE can be undertaken without interfering with the surgical field. Additionally, this imaging can provide a more comprehensive and larger field of view. This latter advantage probably arises from the offset of the transducer from the heart. Still, 3D TEE imaging can be difficult in the near field, especially for visualization of the atria and pulmonary veins.

The following chapter will provide a methodological description of real time 3D TEE in CHD based on the experience to date. Emphasis will be focused on specific clinical examples in which intraoperative 3D TEE imaging can provide additional important information to guide either catheter-based or surgical planning. Additional applications of 3D technology will also be presented.

A note regarding terminology: In the medical literature, both “3D” and “4D” (four-dimensional) are used when referring to 3D echocardiography. The use of the term 4D is

meant to describe the 3D depiction of a moving object (such as the heart), with 3D rendering displayed using real-time motion—thus time represents the fourth dimension. In current ultrasound parlance, the two terms are used synonymously and interchangeably. For simplicity, in this chapter “3D” will be used to represent both terms.

General Concepts

3D TEE Probe Technology

The technology of the current real-time 3D TEE probes was discussed in Chaps. 1 and 2, but will be detailed again in this chapter. The following discussion applies specifically to one device (the Philips X7-2t 3D TEE probe); however, many of the same principles apply to other 3D systems utilizing matrix array technology.

Physically, the 3D TEE probe looks very similar to a standard 2D TEE probe. The same standard TEE handle controls are available—antero-posterior and left-right flexion, as well as a multiplane angle control which rotates the 2D tomographic plane from 0° to 180° (Fig. 19.1a). The 3D TEE probe tip is shaped similar to its 2D counterpart, although it is slightly larger in size (Fig. 19.1b). This larger tip is designed to accommodate the highly advanced, miniaturized technology that makes possible real-time 3D TEE imaging.

The typical 2D multiplane TEE probe consists of a phased array transducer containing 64 piezoelectric crystals (elements) placed side by side in a rectangular row (Fig. 19.2a). As described in Chap. 1, sequential activation of these crystals produces a beam that is steered to obtain a flat, pie-shaped scanning plane. This creates the standard tomographic 2D images customarily seen with the TEE systems currently in use. In a 2D multiplane TEE probe, the rectangular array of elements is physically rotated (electronically or mechanically) in a semicircular manner between 0° and 180° (Fig. 19.2a), thereby obtaining the various 2D TEE tomographic images commonly seen in this and other sources. In contrast, the 3D TEE probe contains a matrix array of 2,500+ piezoelectric crystals arranged in a square 10 × 10 mm grid (Figs. 19.1b and 19.2b). The individual elements are electrically independent, allowing for generation of scan lines that can vary both azimuthally (laterally) and elevationally (Fig. 19.2b). Thus a pyramidal 3D “wedge” of acoustic raw data information can be obtained and subsequently processed into Cartesian coordinates using a 3D scan converter; each discrete point in the scan converter is known as a voxel (“volumetric pixel”), which is cubic in shape and carries a discrete coordinate in 3D space as well as a value for echo intensity [14–16]. This is analogous to the pixels (picture elements) used to form a 2D image. Voxels therefore constitute the basic components used to construct a 3D dataset [5]. Since voxels represent discrete data points,

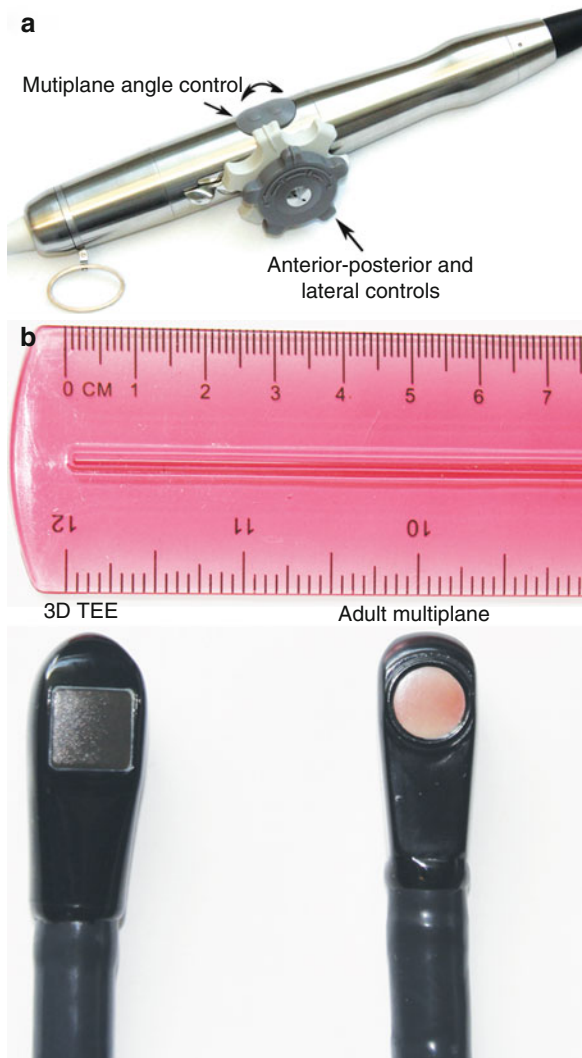


Fig. 19.1 The Philips X7-2t 3D TEE probe. (a) Shows the handle of the probe; it has identical controls as a standard 2D TEE probe. When used for 2D TEE imaging, the multiplane angle control (shown) rotates the imaging plane between 0° and 180° . (b) Is a photo of the Philips adult transesophageal (TEE) 3D and 2D probes side by side. Note that the 3D TEE probe is slightly larger than its 2D counterpart

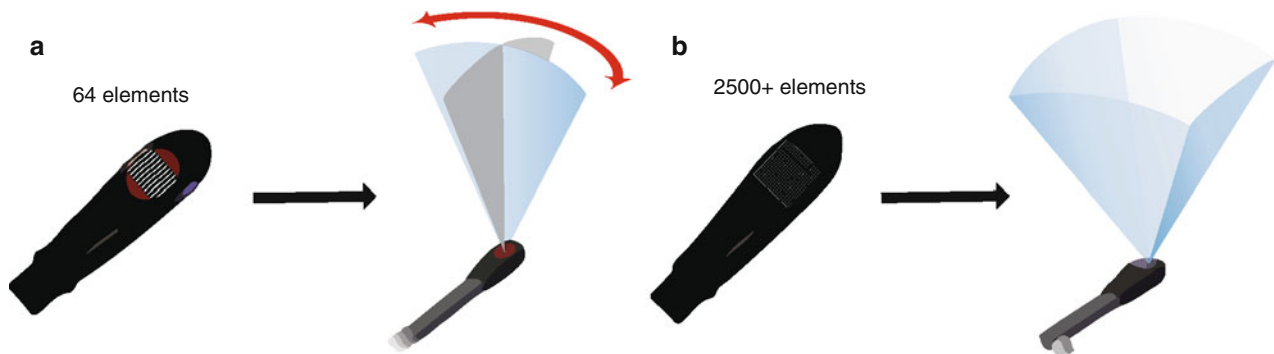


Fig. 19.2 Diagram of adult transesophageal (TEE) 2D and 3D probes. (a) Illustrates a standard multiplane 2D TEE probe, which uses a linear phased array containing 64 piezoelectric elements. Using a control on the TEE probe handle, the array is physically rotated either electronically or mechanically to obtain a multiplane angle between 0° and 180° .

interpolation is used to fill in the gaps between the voxels, using adjacent data of similar characteristics [15]. The resultant 3D image depends upon the size and density of the voxels. Analogous to 2D imaging, smaller voxels and increased number of scan lines lead to a higher voxel count and less data interpolation, which in turn enhances the spatial resolution of the 3D image. However the tradeoff is temporal resolution. There is a large volume of data (several thousand scan lines) that needs to be collected and processed for a single 3D volume dataset, and if the processing of this dataset were performed in a manner akin to standard 2D echocardiography, the time required would result in unacceptably low frame rates. To address this, parallel beamforming (parallel processing) is utilized. In this technique, the system transmits one wide beam and receives multiple narrow beams in parallel [17], which enables much faster 3D image processing, thereby permitting the motion of the 3D images to be displayed at clinically acceptable frame rates. Nonetheless as a result of the greater data processing requirements, the current frame rates for live 3D imaging are still much less than those achievable by conventional 2D imaging. Also, parallel beamforming comes at a cost: there is an accompanying increase in the amount of electronics, as well as size, cost, and power consumption of the system [17].

The process of displaying a 3D data set on a 2D computer screen is known as *rendering*, and can be performed by one of several different methods. The first method, known as *wireframe rendering*, shows the surface of a structure as a series of lines connected together to form a mesh of interconnected polygons that altogether form a cage-like, wireframe 3D model of the surface of the heart (Fig. 19.3a). This method was originally designed for computer-assisted design and manufacturing (CAD/CAM), and is well suited for ventricular wall motion although it cannot display more complex internal structures such as valvular structures [5]. The second method is known as *surface rendering*. Similar to wireframe rendering, surface rendering displays the details

(b) Illustrates a 3D TEE matrix array probe with over 2,500 elements arranged in a square grid. Scan lines are generated both azimuthally (laterally) and elevationally, thus a pyramidal volume can be obtained, enabling the acquisition of a 3D volume dataset

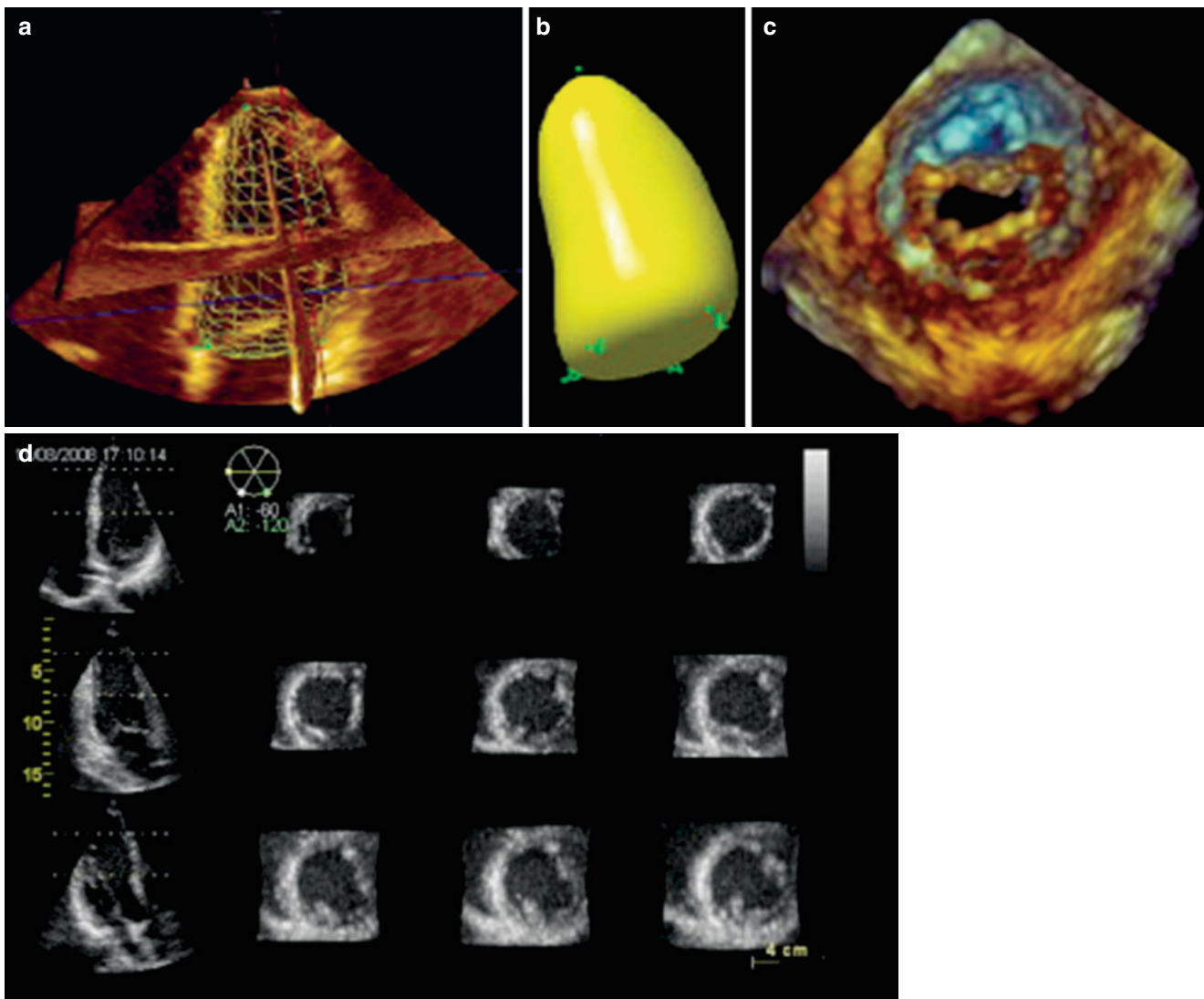


Fig. 19.3 Examples of different modes in which 3D echocardiographic data sets can be visualized and rendered. The techniques used to display the images can be divided into four broad categories: wireframe (a), surface rendering (b), volume rendering (c), and 2D tomographic

slicing (d). These displays were obtained from transthoracic 3D imaging, but the principles of image rendering and display apply equally with 3D transesophageal imaging (Reprinted from Lang et al. [18]; with permission from Elsevier)

of a structure's surface but defines more points to present a solid appearance (Fig. 19.3b). Both wireframe and surface rendering utilize manual tracing or semiautomatic border detection algorithms (identification of blood-tissue boundary) to trace the endocardium in cross-sectional images derived from segmentation of the 3D dataset; these are then used to generate a 3D model of the surface and shape of the structure in question (usually a ventricle). This 3D/4D volume "cast" can then be used for quantification of ventricular volume, synchrony and function [14]. The third method of rendering, known as *volume rendering*, is the method used most frequently in real-time 3D imaging, particularly for the evaluation of structural abnormalities such as those seen in CHD. This method preserves all 3D information within the dataset, and rendering is performed to provide a realistic 3D

depiction of all the anatomic details within the heart. This is achieved by using different algorithms to cast a light beam through the voxels, and weighting the voxels to obtain a voxel gradient intensity. A variety of digital shading and lighting techniques (perspective, light casting, and depth color-coding) are used to achieve the perception of 3D depth and texture on a 2D computer screen (Fig. 19.3c) [18]. Using tools available both on the echocardiography machine as well as offline, these volume datasets can be sectioned (cropped) from any number of different viewpoints, and rotated to reveal the spatial relationships of atrioventricular/semilunar valves and complex intracardiac anatomy. Also, the source of the light beam (and therefore shading/lighting) is projected to maintain a sense of depth and three dimensionality, even while the 3D volume dataset is rotated and

sectioned. Volume rendered datasets can be displayed in four principal modes:

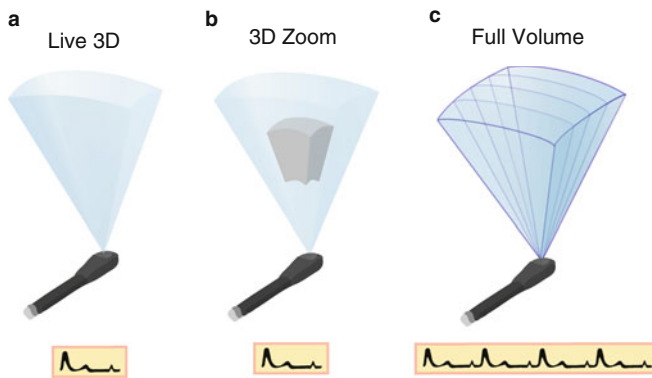


Fig. 19.4 The different modes of volume rendering. (a) Is an illustration showing a Live 3D volume, acquired in one beat and without the need for gating. (b) Shows 3D zoom mode: only data within a small region of interest are acquired, the data are collected in one beat, and no gating is required. (c) Shows a full volume dataset in which four subvolumes that have been sequentially acquired and “stitched” together to form one large volume. Creation of a full volume requires gating to the electrocardiogram

• **Real-time (Live) 3D.** This mode, activated by a single button, provides true live, real-time 3D imaging of the beating heart. However only a portion of the heart is contained in 3D dataset. It is obtained in such a manner that the “front” portion of the dataset (nearest the observer) automatically displays a tomographic slice identical to the 2D image that was shown prior to 3D activation, but with rendered volumetric imaging behind the slice to provide additional information and a 3D perspective (Figs. 19.4a and 19.5, Video 19.1). This 3D mode yields a narrow pyramidal volume with dimensions $30^\circ \times 60^\circ$. Since the “live” format is truly real-time, no gating to respiration or electrocardiogram (ECG) is necessary. However because the structure(s) in question has been “sectioned” to mimic the 2D tomographic image for visualization and orientation, the resultant 3D dataset will not include the entire structure. This mode has a temporal resolution (frame rate) of 20–30 Hz, which is sufficient for monitoring real-time motion and guiding interventional procedures.

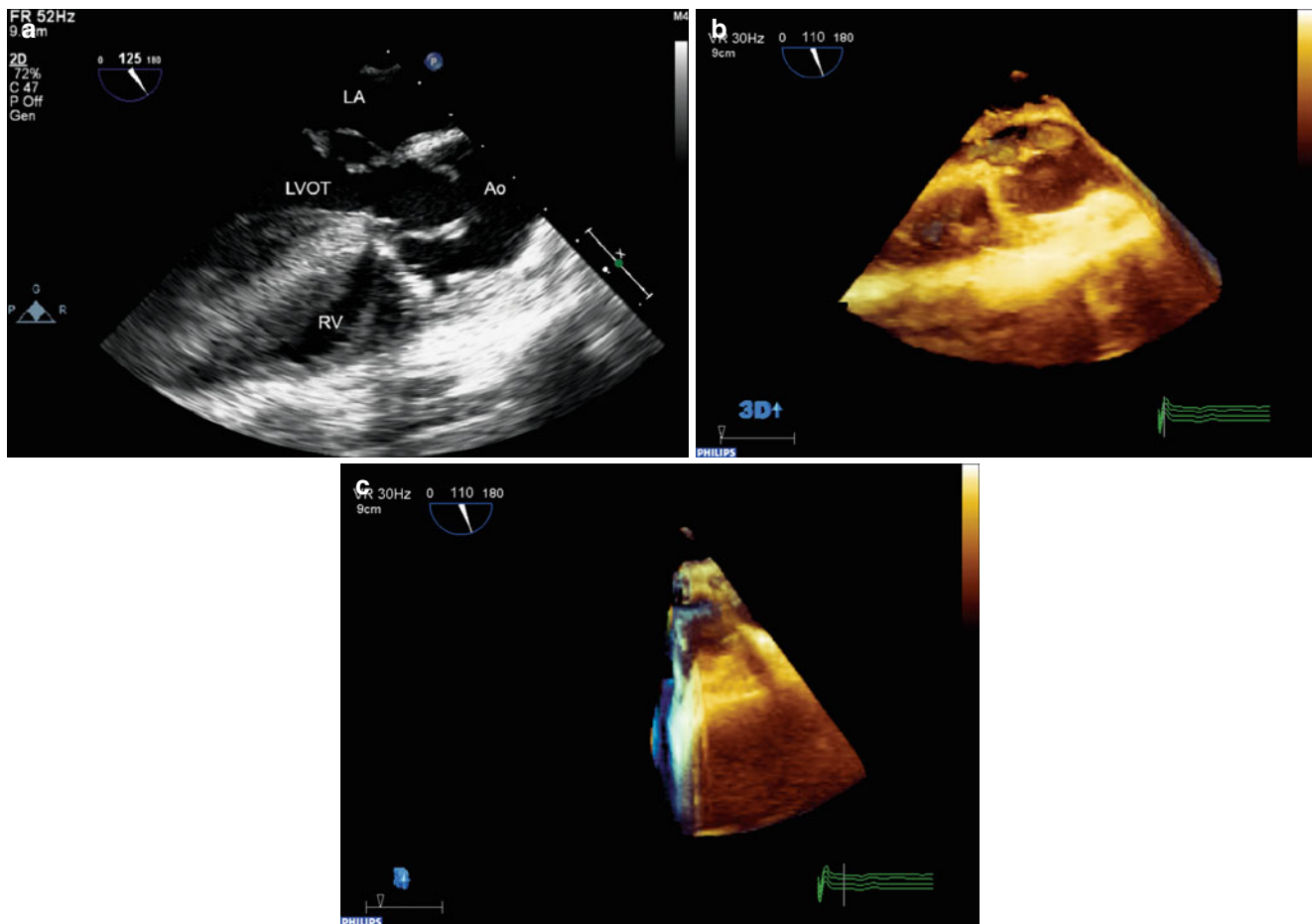


Fig. 19.5 Example of three-dimensional “Live 3D” format in a patient with repaired tetralogy of Fallot and an abnormal aortic valve. A standard mid esophageal aortic valve long axis view (a) was used to position and orient the probe. (b) Shows the “Live 3D” mode volume dataset. Note that the front portion of the dataset displays the tomographic

image similar to the standard 2D image, which helps to orient the echocardiographer. (c) Shows the dataset rotated to show the thickness of the volume. Note that volumetric data is obtained behind the image, but the entire aortic valve is not contained in the dataset. *Ao* aorta, *LA* left atrium, *LVOT* left ventricular outflow tract, *RV* right ventricle

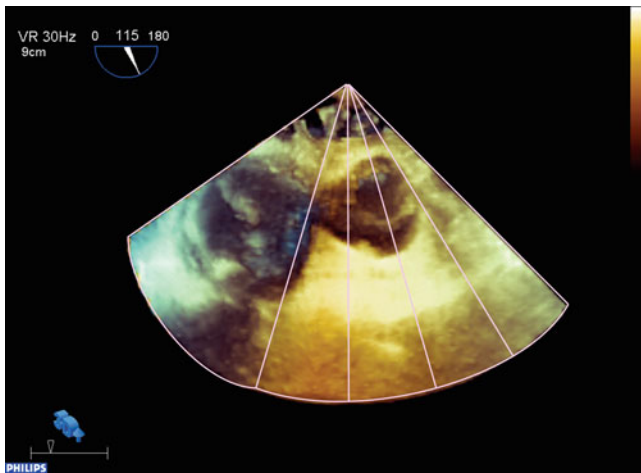


Fig. 19.6 Example of the three-dimensional full volume dataset acquired in the patient from Fig. 19.4. Four subvolumes were collected and rapidly stitched together to form a pyramidal dataset. Now a significant portion of the heart, including the whole aortic valve, is contained in this dataset. The volume has been rotated from its initial acquisition display, and lines have been drawn to illustrate the manner in which the subvolumes are collected and stitched together

- 3D Zoom.** This mode is also a “live” mode. A specific region of interest (e.g. the mitral valve) is identified, and a smaller volume dataset positioned to provide a focused, magnified, complete 3D visualization of the region as a smaller and narrower pyramid (Fig. 19.4b). The pyramid angles can vary from $20^\circ \times 20^\circ$ to $90^\circ \times 90^\circ$, with a dimension of $30^\circ \times 30^\circ$ commonly used. By reducing the volume size and focusing solely upon the structure of interest, the entire structure can be contained in the dataset, and the lateral resolution can be improved by increasing the number of scan lines, while still maintaining acceptable frame rates. The live images can still be cropped and rotated in multiple orientations. However progressive increasing of the magnification can produce deterioration in both spatial and temporal resolution (sometimes down to 5–10 Hz) [18].
- 3D Full Volume.** This is a gated acquisition mode in which a large 3D volume dataset is assembled from several adjacent wedge-shaped 3D subvolumes that are collected rapidly and sequentially using ECG-gating. A total of 4–7 subvolumes are obtained and then digitally reassembled or “stitched” into a large pyramidal digital dataset, which is then available for viewing and manipulation (Figs. 19.4c and 19.6, Video 19.2). Strictly speaking, a full volume dataset is not real-time since it represents an ECG-gated assemblage of subvolumes collected sequentially over a matter of seconds, but for all practical purposes it is nearly so because of the very short acquisition and display time. This mode provides excellent spatial and temporal resolution (20–50 Hz, depending upon number of beats captured), and because of the wide

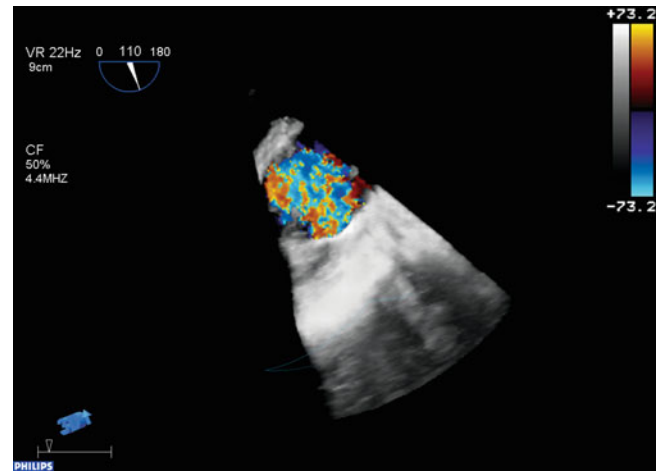


Fig. 19.7 Example of a three-dimensional color flow dataset in the same patient in Figs. 19.5 and 19.6. Turbulent systolic flow is noted across the aortic valve

dimensions of the volume dataset ($90^\circ \times 90^\circ$), entire structures can be completely captured within the dataset. However due to the gating, full volume datasets can be subject to “stitch” artifact (imperfect alignment of subvolumes) if there is significant respiratory motion or any ECG abnormality.

- 3D Color Doppler.** 3D color flow Doppler volume datasets can also be obtained, with the 3D color Doppler information superimposed upon the 3D image information (Fig. 19.7, Video 19.3). These 3D color flow volume datasets are assembled from 7 to 14 thin ECG-gated subvolumes in the same manner as the full volume datasets described above, although they smaller than the full volume datasets. Due to the many subvolumes required, some degree of stitch artifact is not uncommon with these datasets. Also, temporal resolution tends to be reduced (<10 Hz). During post-acquisition review, the dataset can be viewed as only imaging, only color Doppler, and with color Doppler superimposed upon the image, similar to standard 2D/color flow imaging.

Newer 3D software now enables a larger volume of scanning while performing live 3D imaging; often the size of the volume approaches that of the stitched full volumes detailed above. This is termed “single beat” full volume scanning, and does not require ECG-gating; hence it is not subject to artifacts from arrhythmias. However there is a tradeoff, as less information (due to lower frame rates) is available for this single beat. For improved resolution, more data must be obtained over several successive ECG-gated beats (2, 4, or 6), thus replicating the process of the stitched full volume acquisition. The newer software also allows real time 3D color Doppler scanning to be performed, though frame rate decreases appreciably. Again, this can be improved with acquisition over multiple ECG-gated beats. With both the

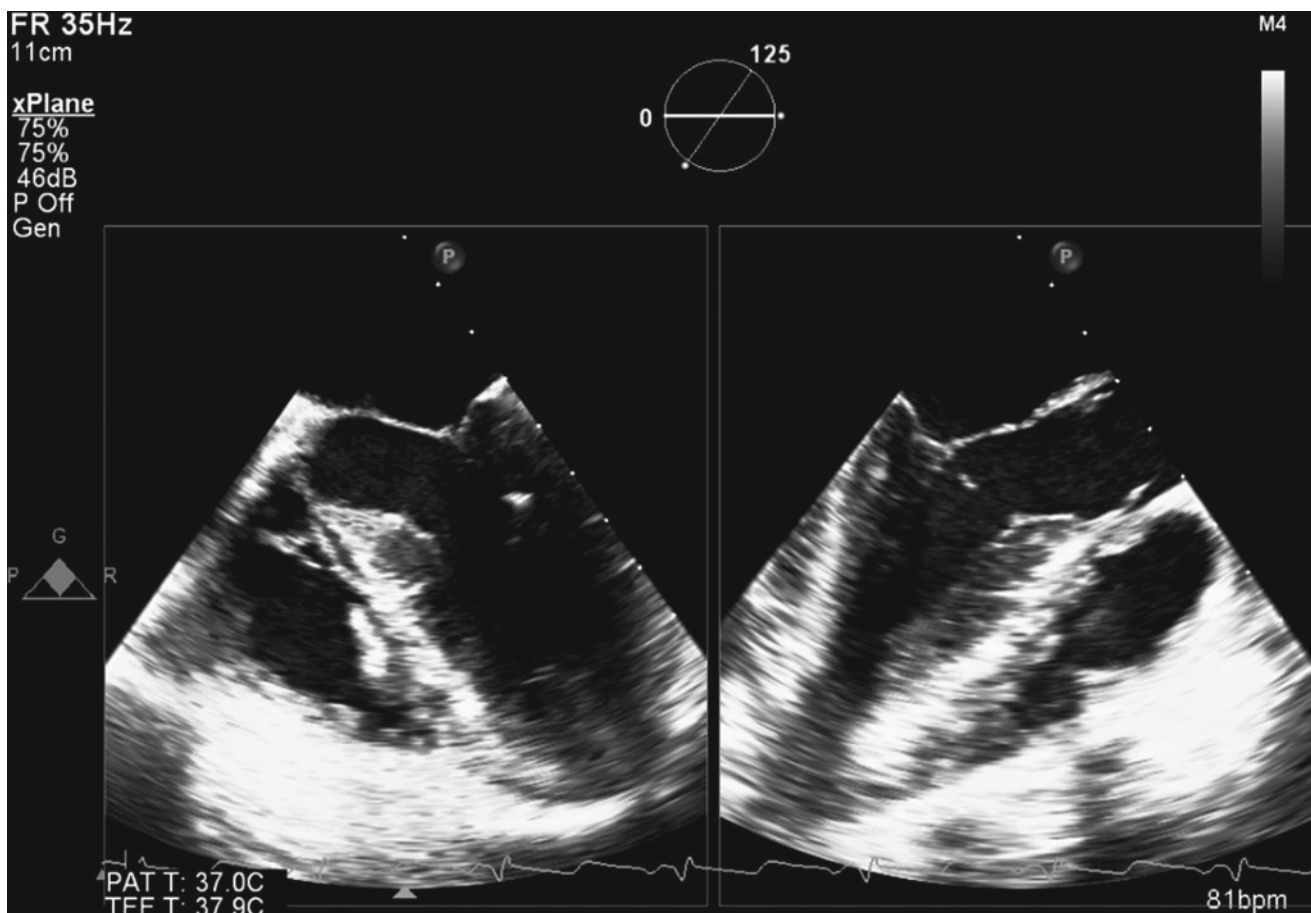


Fig. 19.8 xPlane mode from the Philips X7-2t 3D TEE probe. Two different 2D planes are shown simultaneously in this patient with mild subaortic stenosis. On the left is a mid esophageal four chamber view,

on the right a mid esophageal long axis view. The circle on the display indicates the relationship of the two planes

single beat full volume imaging as well as color flow Doppler modes, the selection of an increasing number of ECG-gated beats produces incremental improvements in frame rates, but the potential for stitch artifact also increases.

In addition to its 3D capabilities, the 3D TEE matrix transducer can also function as a standalone 2D multiplane probe, with full 2D, color flow and spectral pulse/continuous Doppler as well as M-mode capabilities (tissue Doppler imaging is available in later software releases). Like a standard 2D TEE probe, the tomographic plane position can be steered between 0° and 180° using a control on the probe handle (Fig. 19.1a). However, unlike a 2D TEE probe, no physical motion of the elements actually occurs at the probe tip—instead the tomographic plane is electrically steered by coordinated activation of the matrix elements to vary scan lines and obtain a multiplane angle between 0° and 180°. Moreover, one of the unique features of the matrix array is that several different 2D tomographic planes can be displayed simultaneously from the same volume dataset, a feature variously known as biplane, triplane, or multiplane imaging (Fig. 19.3d). These can be displayed as equidistant

parallel slices (as shown in Fig. 19.3d), three orthogonal planes together, or slices rotated around a common axis. For example, with the Philips 3D TEE system, two different live 2D images can be displayed next to each other using the xPlane mode, as shown in Fig. 19.8, Video 19.4. In this example, mid esophageal four chamber and long axis views are shown simultaneously. Multiplane imaging from a 3D volume dataset has been shown to be useful when evaluating CHD [19].

Advantages of Real-Time 3D TEE

With conventional 2D imaging, the tomographic planes, once acquired, cannot undergo further alteration of the views. Instead, further images must be collected by various TEE probe maneuvers and multiplane angles (Chap. 4) to provide additional visualization of a structure in question. The advantage of real time 3D TEE is the immediate manner in which the volume datasets are available for analysis, and the multiple ways in which a dataset can be manipulated to

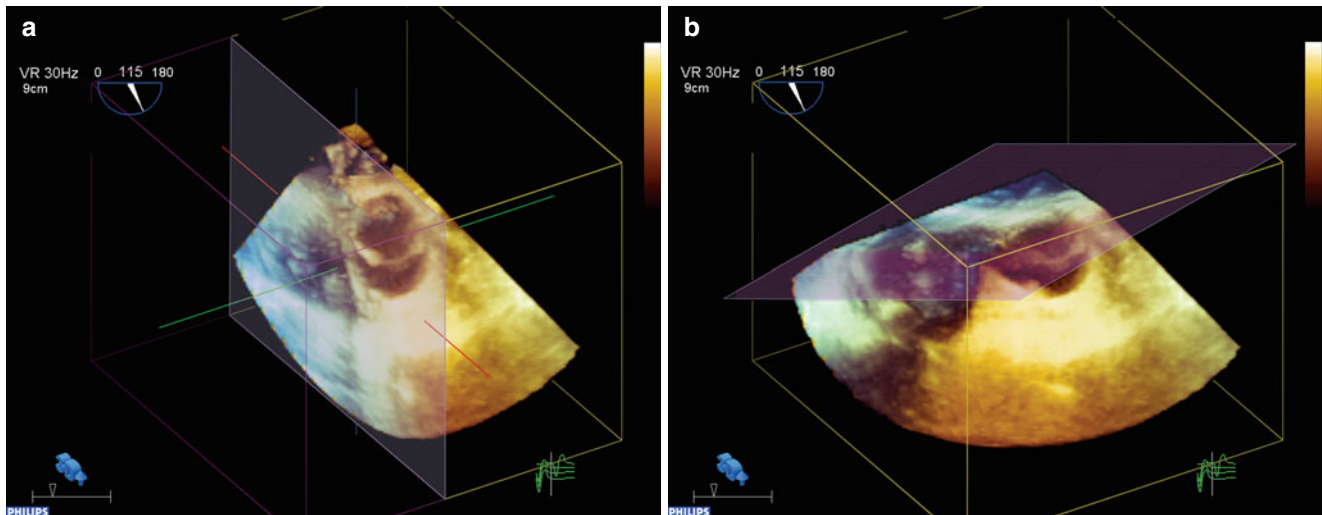


Fig. 19.9 Example of cropping of a full volume dataset in the patient from Figs. 19.4 and 19.5. (a, b) Show the full volume dataset cropped in different planes: one of the standard perpendicular (x,y,z) cropping

planes (a), and an “anyplane” cropping mode that can be performed from any angle (b). The latter can be used to visualize the intracardiac anatomy from a multitude of different perspectives

yield novel anatomic perspectives not visible by 2D imaging. Two important maneuvers are used to evaluate a rendered 3D dataset; these maneuvers are unique to 3D imaging, and not used for 2D imaging. The first maneuver is **cropping**, in which a flat plane can be used to section the heart from any desired angle or perspective (Fig. 19.9, Video 19.5). This maneuver “crops away” a portion of the heart adjacent to the structure of interest, thereby enabling enhanced visualization of the structure, often in a manner or from a vantage point that cannot be provided by conventional 2D imaging. Examples of this include an *en face* view of the atrioventricular valves, or an *en face* view of an atrial or ventricular septal defect. The second maneuver is **rotation**: the dataset can be rotated (cropped or uncropped) in any direction to provide different views of the structure in question from a number of perspectives, e.g. visualization of an atrial septal defect, first from right atrium, then from the left atrium. Rotation enhances the understanding and appreciation of the 3D layout of the cardiac structures. Together, cropping and rotation enable the examiner to perform a “virtual dissection” of the heart. For those observers less familiar with the more unconventional cropped views, a 3D volume dataset can also be cropped and rotated to provide images that resemble their analogous (and more recognizable) standard 2D TEE images. Moreover, the multiplane 2D mode allows production of simultaneous high quality 2D TEE images, which are sometimes more familiar to viewers (Fig. 19.8, Video 19.4). Dataset viewing and manipulation can be performed directly on the echocardiography machine, or subsequently offline on a computer workstation equipped with 3D rendering/analysis software.

At our center, we first evaluate the area of interest in a “live” 3D TEE format. This mode allows for changes in threshold

and gain settings with immediate feedback. Using the live data sets for transducer orientation, the full volume data sets are then obtained. Respiration is suspended by the anesthesiologist during the acquisition phase. This acquisition phase is short, i.e. four to eight cardiac cycles, and does not create respiratory/cardiac compromise. With experience, the echocardiographer can perform rapid manipulation and analysis of both live and full volume 3D TEE datasets at the bedside; specific cardiac abnormalities can be immediately segmented and displayed for the surgeon. The full volume acquisitions in particular provide a broad, encompassing display of large portions of the heart. This can enable an excellent display of the anatomy and spatial relationships of the various cardiac structures.

3D Image Display

At our center we have developed specific anatomic displays of the 3D images. We have found this to be important for several reasons. First, this establishes the underpinnings of the anatomic display to enhance understanding and communication between the surgeon, cardiologist and anesthesiologist. In particular, we strive to portray the 3D images similar to the view or perspective of the cardiovascular surgeon. Second, with experience we have learned the specific cut planes that best depict the optimal imaging information for the specific defects. Third, with time, we believe this will establish a more universal or ubiquitous imaging display orientation to enhance understanding and communication with other imaging centers, cardiologists and surgeons.

As mentioned above, the imaging planes have been established to simulate the surgeon’s perspective of the anatomic defect. For example, if displaying the mitral valve from

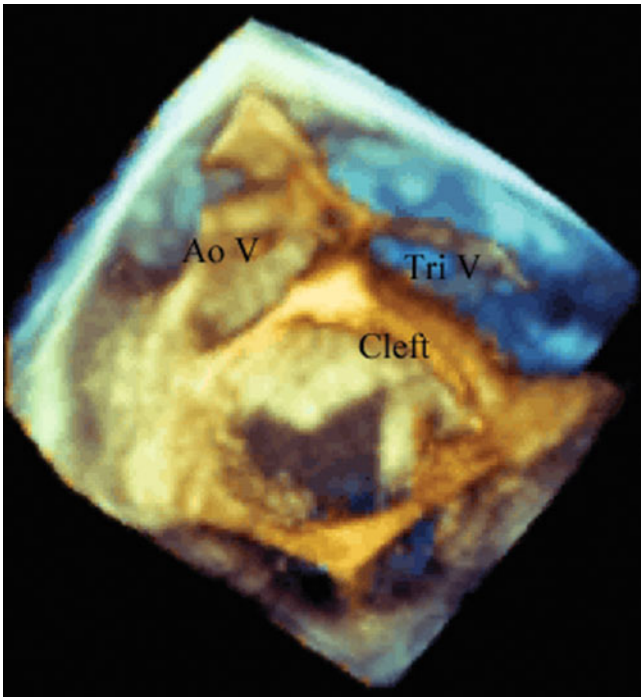


Fig. 19.10 Left atrial view imaging the superior surfaces of the left atrioventricular valve in a 23 year old woman who had previous closure of a primum atrial septal defect and had progressive left atrioventricular valve regurgitation. The aortic valve or superior aspect of the heart is to the left, and the anterior aspect, tricuspid valve, is to the top of the screen. During diastole a significant residual cleft in the anterior leaflet is easily seen, with thickened leaflet edges. *Ao V* aortic valve, *Tri V* tricuspid valve

above, i.e. atria, the anterior aspect is to the top of the screen and the more superior aspect to the left. This will place the anterior leaflet to the superior/leftward aspect of the monitor screen, and the mural or posterior leaflet to the right/inferior aspect of the monitor, (Fig. 19.10, Video 19.6).

Again, to establish conventional imaging planes, the aortic valve is displayed similar to the surgeon's view as if looking from the aortic root onto the superior aspects of the valve (Fig. 19.11, Video 19.7a and 19.7b). Thus, the right coronary leaflet is to the top, and the left coronary leaflet is to the left and inferior. The non-coronary cusp is to the right and inferior. Creating these specific-anatomic orientations is essential for optimal communication with the surgeon.

The transducer orientation depends on the specific anatomic abnormality. Naturally for the aortic valve the transesophageal imaging plane is set to obtain good short and long axis views. Both live and full volume gray scales, as well as color flow full volume acquisitions, are obtained in both the short axis and corresponding orthogonal imaging planes. One might argue that orthogonal image acquisitions would not seem to be necessary in that all the information should be within the full volume data set. If optimal temporal and spatial gating is met, imaging artifacts should not be

present regardless of the segmentation planes. Nonetheless spatial artifacts can be present, and some will be more apparent depending upon the acquisition orientation.

3D TEE for CHD Evaluation

Considerations for 3D TEE in the Evaluation of CHD

One of the most often asked questions is: which patients should get a 3D echocardiographic study, in addition to standard 2D imaging? This is especially germane to 3D TEE imaging, which requires some additional effort compared to 2D TEE imaging. At our center, the surgeon most often requests 3D echocardiographic imaging especially for valve repairs [20–23]. Beyond this straightforward answer, 3D imaging is applied to particular congenital heart abnormalities in which a 3D perspective would provide important additional information in addition to 2D imaging. Another 3D TEE application includes imaging in certain congenital defects that have often required multiple re-operations. Hence any imaging that might be useful in providing information to the surgeon to enhance the repair and prevent re-operation would be advantageous. This certainly would apply to congenital heart defects such as complex atrioventricular canal defects [6], complex left ventricular (LV) outflow tract obstructive lesions [24], or repair of Ebstein anomaly of the tricuspid valve [25]. As discussed below, 3D TEE has proven application for catheterization closure of atrial and ventricular septal defects [26–29]. It provides important spatial imaging that can significantly enhance anatomic assessment of these defects. Furthermore, it can provide real-time information during the device deployment procedure, thereby guiding more precise device placement, and helping to reduce fluoroscopic imaging time.

The currently available real-time 3D TEE probes are relatively large, and their use in pediatric patients is limited by patient size. They are suitable primarily for older children and adolescents >25–30 kg, although successful probe insertion down to 15.5 kg has been reported [13]. Nonetheless even in older patients with CHD, 3D TEE has found widespread utility in a number of different clinical settings. For example, 3D TEE imaging is readily applicable in the catheterization laboratory. This applies not only for visualization of the atrial and ventricular septal defects for device closure, but also for detection of thrombus formation for patients considered for electrical cardioversion. In the ambulatory setting, 3D TEE can be used for the adolescent or adult patient in whom surgery is contemplated, when transthoracic imaging is suboptimal and cardiac MRI imaging either not feasible or contraindicated. Thus, a patient may undergo a 3D TEE study to determine the feasibility of either catheterization or surgical based intervention. Naturally, 3D TEE is also

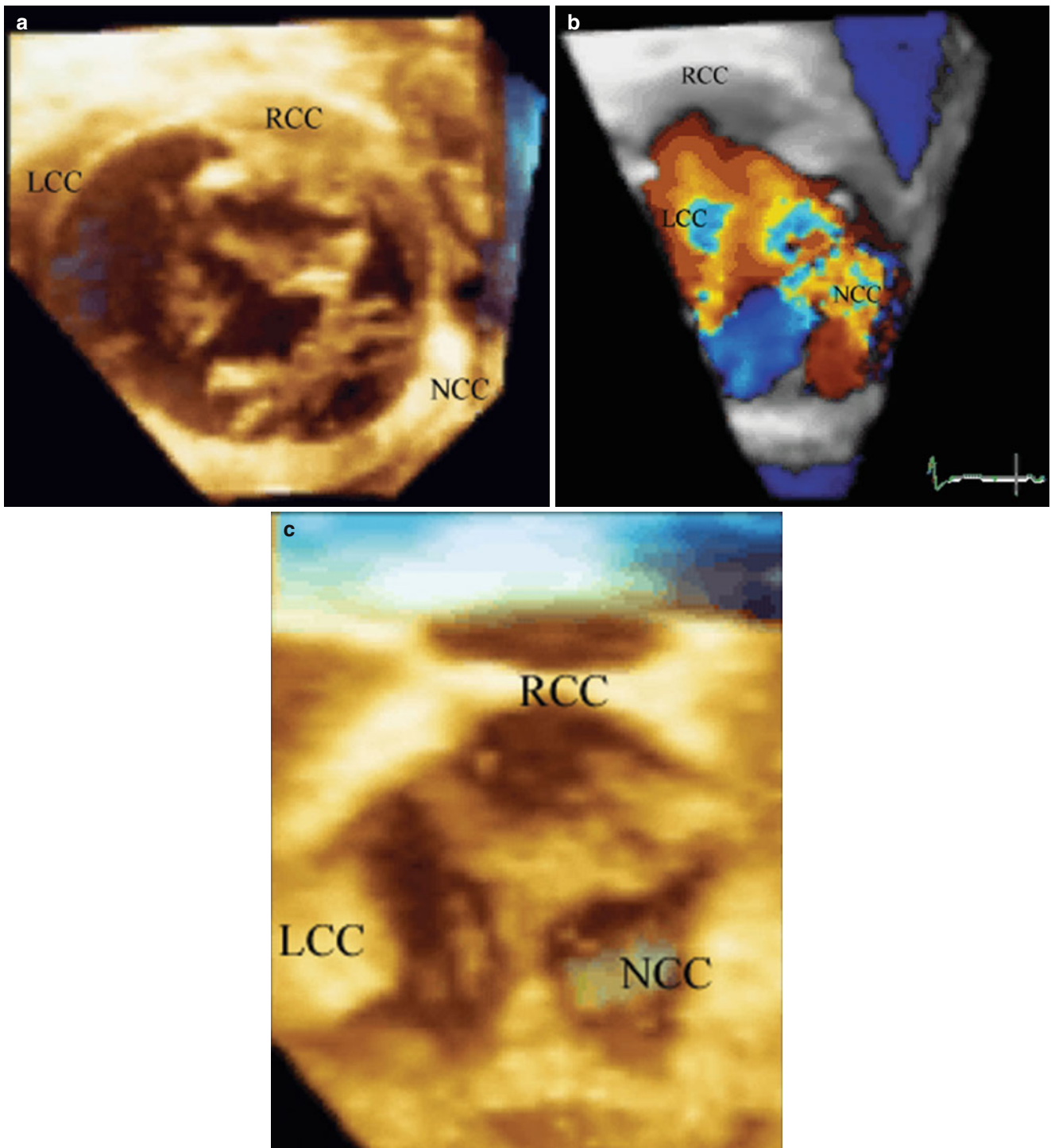


Fig. 19.11 A 12 year old with severe aortic regurgitation. Images are constructed to view the superior surface of the aortic valve as if looking from the aorta down on to the leaflets. To the top is the right coronary cusp, to the left the left coronary cusp, and to the right is the non-coronary cusp. (a) Is obtained during the pre-bypass period and shows the marked lack of coaptation and resulting area of regurgitation due to the retracted,

scarred non-coronary cusp. (b) Verifies color protruding through the region on the regurgitant orifice area of the non-coronary cusp. The patient had pericardial replacement of the non-coronary cusp, and pericardial extension of the right and left coronary cusps. The resultant post bypass 3D echo. (c) shows excellent coaptation of all three leaflets. *LCC* left coronary cusp, *NCC* non-coronary cusp, *RCC* right coronary cusp

used in the operative setting. Often 3D TEE has better imaging resolution than transthoracic 3D echocardiography, hence the preoperative study serves a vital role by providing important imaging planes for the surgeon to aid in the planning of the operation. Postoperatively, this imaging can be applied during separation from bypass to evaluate the success of the surgery.

Clinical Application for 3D TEE in the Evaluation of CHD

Much of the published literature on the subject of 3D echocardiography for CHD evaluation is based upon extensive experience with real-time transthoracic (and even fetal) 3D echocardiography [30–36]. However, the matrix array technologies for real-time transthoracic and transesophageal 3D echocardiography are very similar, and therefore one can expect considerable overlap between the two modalities in terms of clinical applications. The major advantage of 3D TEE is the enhanced resolution of the 3D images, particularly in larger patients with poor transthoracic windows. Furthermore TEE is typically performed in more controlled clinical settings (often intubated patients undergoing general anesthesia), thus permitting better acquisition of full volume datasets. Thus there is a growing body of literature documenting the expanding clinical applications of 3D TEE for CHD evaluation [13, 36–39]. Up to the present time, most of these applications focus upon structural/morphologic evaluation of CHD, primarily in the intraoperative and interventional catheterization settings (as befits the most common venues for TEE in this setting). In this section, some of the more common clinical applications will be discussed. Not all applications of 3D TEE can be presented; however, examples of specific CHD abnormalities most commonly evaluated will be discussed below.

Evaluation of Atrioventricular Valves

Evaluation of the atrioventricular valves represents one of the most well-established indications for 3D echocardiography in adults and children. A number of studies have documented the utility of both transthoracic and transesophageal 3D echocardiography, especially for mitral valve disease in adults [18, 20, 40, 41]. In particular, 3D echocardiography enhances the anatomic visualization of all levels of the atrioventricular valve—leaflets, chordae, and papillary muscles. Moreover 3D echocardiography is able to display the valve in a manner unavailable by 2D echocardiography, including the *en face* “surgeon’s view” as described above. In adults,

3D TEE provides a realistic and detailed *en face* visualization of the individual mitral valve anterior leaflet segments and posterior leaflet scallops [40]. The same holds true for congenital atrioventricular valve abnormalities, in which 3D echocardiography (primarily transthoracic, but also TEE) has proven very useful, particularly for endocardial cushion defects (atrioventricular septal defects) and Ebstein anomaly of the tricuspid valve [6, 25, 42, 43]. A number of studies have also discussed the use of 3D echocardiography for evaluation of mitral valve disease due to parachute mitral valve [44], double orifice mitral valve [45, 46], mitral valve arcade [47], and congenital mitral regurgitation as well as other mitral valve anomalies. There have also been some recently published studies evaluating the utility 3D echocardiography (both transthoracic and TEE) for more precise evaluation of the pathology of congenital atrioventricular valve abnormalities, specifically in regard to mechanisms and sites of valve regurgitation [32, 47]. Some examples of 3D TEE for assessment of congenital atrioventricular valve abnormalities will be discussed below.

Despite excellent surgical results for endocardial cushion defects, a disquieting number of patients require re-operation for left atrioventricular valve stenosis or regurgitation. In patients that require re-operation for valve regurgitation, 3D imaging provides an excellent perspective of residual regurgitation via clefts in the anterior leaflet, (Fig. 19.10, Video 19.6). The length and position of the residual cleft can be depicted, as well as the precise zones of leaflet prolapse. Intraoperative 3D TEE imaging is used pre and post bypass to evaluate the anatomic extent of residual cleft and associated potential stenosis or regurgitation. Figure 19.10 shows the 3D display, similar to the surgeons viewing, i.e. imaging the superior surfaces of the left atrioventricular valve from the left atrium.

Our center has recently embarked on the “Cone” procedure to improve surgical repair of Ebstein malformation of the tricuspid valve [48]. Previous types of valve repair for this anomaly have been associated with variable success [49, 50]. In part, this has been predicated on preoperative imaging that has, to date, not clearly depicted the anatomic abnormalities. The very complex and variable anatomy of Ebstein malformation does not allow for optimal imaging in a standard 2D display. For example, in the most severe form of Ebstein malformation the leaflet structures are displaced anterior and superiorly towards the right ventricular (RV) outflow tract. The long and ample anterior leaflet envelops the RV as it attaches to the infundibulum. This is often unappreciated by 2D imaging, but can readily be appreciated from full volume 3D echocardiographic data sets obtained

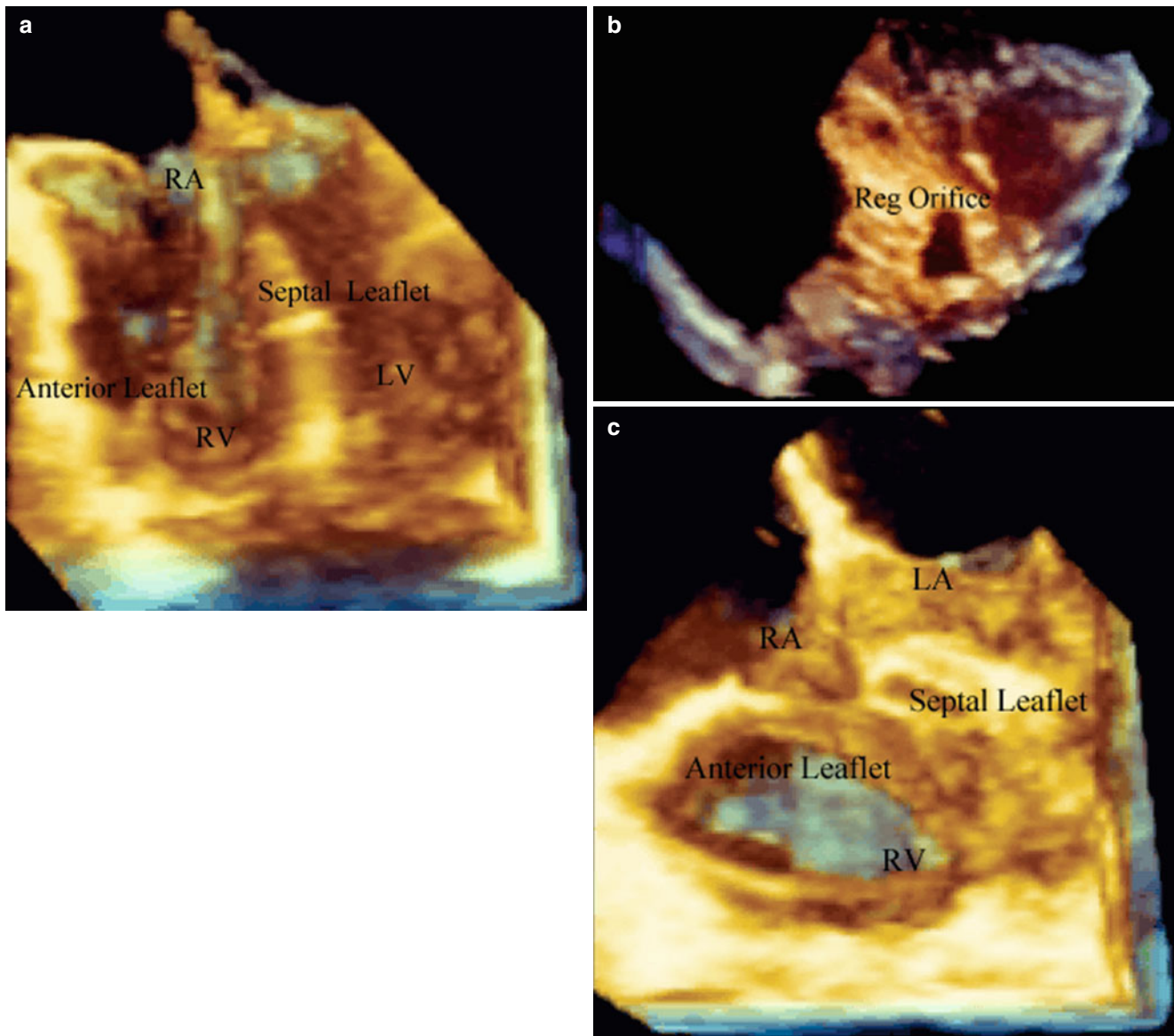


Fig. 19.12 Ebstein malformation of the tricuspid valve. (a) Is a four chamber view of the heart oriented anteriorly and shows a very large anterior leaflet and severely tethered septal leaflet. (b) Is a short axis plane oriented from the RV apex to base of the heart demonstrating a very large zone of non-coaptation (*Reg Orifice*). (c) Is a post-bypass

image in the same patient in (a) after the cone operation. The entire leaflet structure now folds together during systole without a region of non-coaptation. *LA* left atrium, *LV* left ventricle, *RA* right atrium, *Reg Orifice* regurgitant orifice, *RV* right ventricle

from 3D TEE studies (Fig. 19.12, Video 19.8a and 19.8b) [25]. Moreover, unusual clefts, and attachments from the RV free wall to the anterior leaflet are well appreciated with 3D TEE (Fig. 19.12a, Video 19.8a). Often a large zone of the regurgitant orifice area can readily be depicted from short axis planes oriented from apex to base (Fig. 19.12b, Video 19.8a). Similar to aortic and mitral valve repairs, a more dynamic and complete depiction of tricuspid valve leaflet structure and coaptation can readily be seen from 3D TEE after separation from bypass in the operating room (Fig. 19.12c, Video 19.8b).

In addition to native atrioventricular valve pathology, 3D TEE has been found to be useful for the evaluation of prosthetic atrioventricular valves (primarily prosthetic mitral valves) [51]. It allows detailed assessment of valve dehiscence and clot formation. 3D color is especially helpful when evaluating for perivalvar leaks [15, 52].

Evaluation of Semilunar Valves

Aortic valve repair rather than replacement is often preferred in the pediatric patient for obvious reasons. Transesophageal and epicardial 3D echocardiography have become useful for

the pre-operative assessment of the pediatric or adolescent patient with aortic valve disease being considered for valve repair [7, 13]. 3D TEE provides important information to determine the precise etiology of valve regurgitation (Fig. 19.11a, Video 19.7a). The specific anatomic defect can be seen, and 3D color flow can be applied to further confirm the abnormality (Fig. 19.11b, Video 19.7a). 3D imaging provides not only for more precise depiction of commissural fusion, but also the more exact site and extent of lack of leaflet coaptation. More importantly, 3D imaging can provide a perspective as to the depth of the valve leaflet, and hence effective areas of leaflet coaptation. 3D TEE can be immediately applied during separation from cardiopulmonary bypass to analyze the integrity of the aortic valve repair (Fig. 19.11c, Video 19.7b). This modality demonstrates the effectiveness of leaflet coaptation and opening, visualizing the depth of leaflet integrity. As seen in Fig. 19.11a–c and Video 19.7a and 19.7b, the 3D echocardiographic images were oriented to simulate the surgeons view, depicting the valve as looking inferiorly (from the examiner's perspective) onto the superior surfaces of the aortic valve leaflets as if viewed from the aorta.

In adult patients with aortic valve stenosis and/or regurgitation, 3D TEE has been shown to provide anatomic detail regarding valve leaflet morphology and function [41, 53, 54]. Furthermore, the ability to obtain *en face* views of the valve (both above and below the valve) enables the direct planimetry of the aortic valve orifice area [55] in cases of stenosis, or vena contracta/regurgitant orifice area in aortic valve regurgitation [56]. The information from 3D TEE can be used to complement that from 2D TEE imaging, 2D color flow, and spectral Doppler assessment of the aortic valve (Chap. 11). Combining Doppler velocities of the LV outflow tract (obtained from transgastric or deep transgastric views) with the cross-sectional area of the outflow tract obtained by direct planimetry of the 3D TEE image enables a more accurate calculation of aortic valve area when using the continuity equation. A number of investigators have found the LV outflow tract to be ellipsoid rather than circular in shape, when directly measured by 3D echocardiography (transthoracic or TEE) [18, 57–59]. Thus the use of 3D echocardiography likely results in a more accurate calculation of aortic valve area than the method commonly used with 2D echocardiography [60].

There is little information currently available in either the pediatric or adult literature on the use of 3D echocardiography (transthoracic or TEE) for the evaluation of congenital pulmonary valve pathology. One report using transthoracic 3D echocardiography in adult patients with congenital RV outflow tract abnormalities demonstrated that the pulmonary valve could be visualized in 70 % of patients, but the RV outflow tract in only 40 %. However the anatomic findings, when visible, were useful [61].

Evaluation of Atrial and Ventricular Septal Defects

Evaluation of atrial and ventricular septal defects represents a very important clinical application for 3D echocardiography. This is especially true because of the unique *en face* views of the atrial and ventricular septa that are provided by cropping the 3D datasets; these views can greatly enhance the understanding of the morphology and extent of the cardiac defects [29, 62–67]. This information is invaluable when planning and performing (monitoring) interventional catheterization procedures [11, 28, 68, 69]. Because of the proximity of the TEE probe to the atrial and ventricular septa, 3D TEE often provides a significantly greater amount of detail compared to transthoracic 3D imaging. Thus 3D TEE is a natural “fit” for interventional catheterization procedures involving the atrial and ventricular septa. As mentioned, 3D TEE imaging can be applied to atrial septal defect closure in the catheterization laboratory. The full circumference of the atrial septal defect can be imaged from the left and right atrium. These *en face* views allow for depiction of the defect, surrounding rims, as well as the spatial orientation to other anatomic structures (Fig. 19.13a, b; Video 19.9a and 19.9b). In conjunction with live transesophageal imaging, the procedure of closing the defect can be seen from a 3D perspective. This includes the placement of the sheath in the left atrium as well as unfolding of the device in the left atrium. Under simultaneous visualization, the orientation of the disc to the left atrial surface can be seen in a 3D perspective as the device is maneuvered to the left atrial surface (Fig. 19.13c, Video 19.9c). The surface of the disc to the left atrial surface can be depicted prior to deployment. After the left and right atrial discs are deployed, a direct *en face* view of the disc can be seen to verify the appropriate position (Fig. 19.13d, Video 19.9d).

The advantages that 3D TEE confers to atrial septal defect closure also apply to device closure of ventricular septal defects (both percutaneous and perventricular). 3D TEE assists in all phases of the intervention: from pre-procedure evaluation of defect morphology, to catheter positioning and monitoring of device delivery, to relationship of the deployed device to ventricular septum prior to release, and finally device evaluation following complete release. Only a few studies have yet been published on the use of 3D echocardiography (transthoracic and TEE) for ventricular septal defect device closure [33, 70, 71]. However, given that standard 2D TEE is already an integral part of these procedures [72–78], it seems likely that 3D TEE can only serve to provide additive value in those patients of sufficient size to accommodate the larger probe.

In the intraoperative setting, 3D TEE can provide incremental value in the preoperative assessment of ventricular septal defects prior to surgery. As noted above, 3D TEE

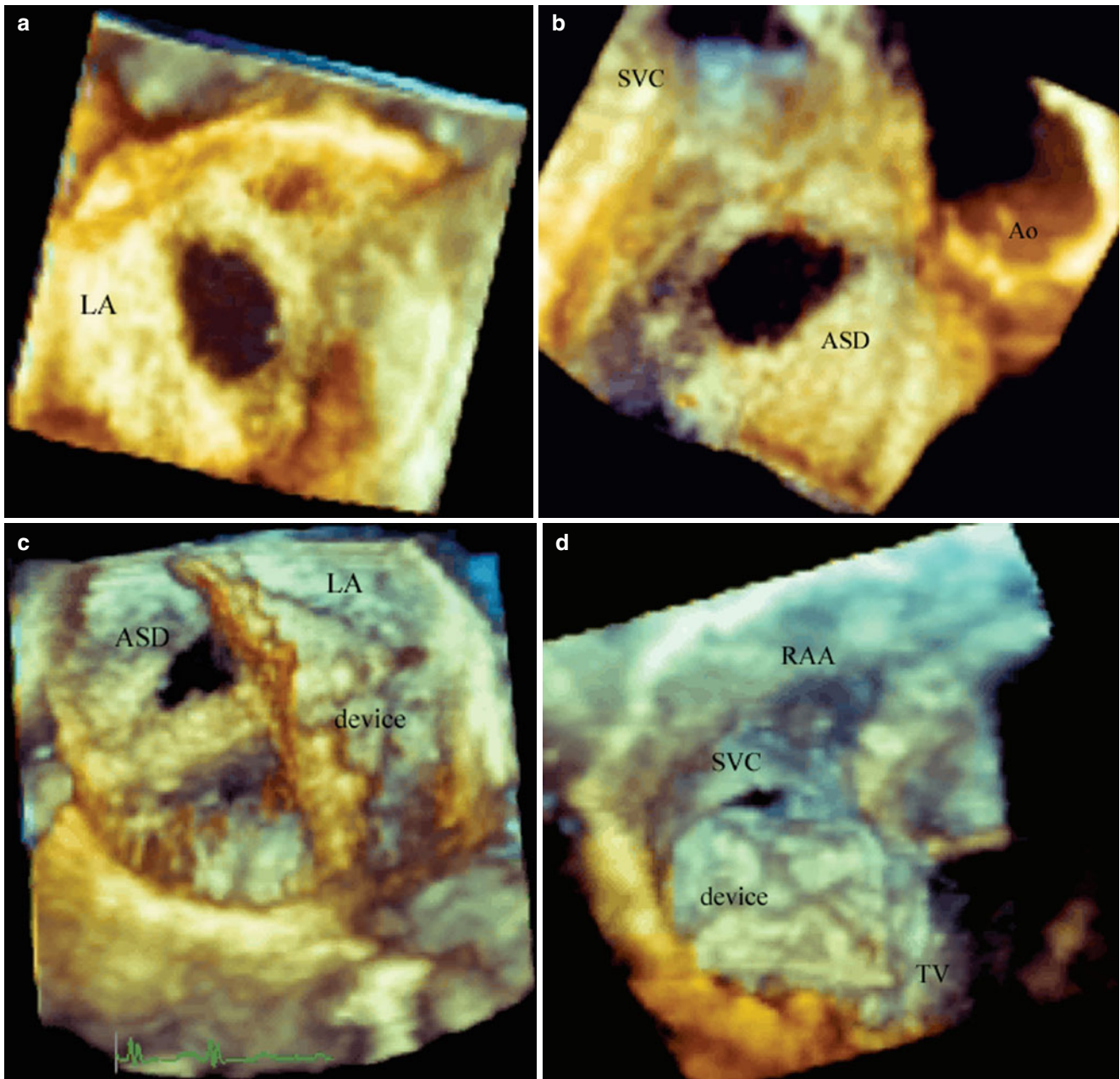


Fig. 19.13 Catheterization device closure of a secundum atrial septal defect. (a) Is a Full volume acquisition displaying an *en face* view of a secundum atrial septal defect from the left atrium. (b) Is a Full Volume acquisition of the atrial septal defect from the right atrial side demonstrating the relationship to the aorta and superior vena cava. (c) Is a live

acquisition from the left atrial view demonstrating the sheath placed through the defect and the left atrial disc deployed within the left atrium. (d) Is an *en face* view of the right atrial disc after being deployed. ASD atrial septal defect, Ao aorta, LA left atrium, RAA right atrial appendage, SVC superior vena cava, TV tricuspid valve

enables visualization of ventricular septal defects in unique *en face* imaging planes not available by standard 2D imaging (Fig. 19.14, Video 19.10). Although 3D TEE might not seem to add significant additional clinical information for surgical closure, certain unusual defects may need a better definition of the spatial relations of the defect to other anatomic structures. Figure 19.15 is taken from a young adolescent followed for many years with a restrictive ventricular septal

defect. Although suspected by 2D imaging, 3D TEE provided additional imaging projections to improve understanding of the hemodynamic abnormalities. Figure 19.15 and Video 19.11 show the 3D TEE aspects of severe prolapse of the right coronary cusp of the aortic valve through a doubly committed subarterial ventricular septal defect. The prolapse was so severe that it created moderate RV outflow tract obstruction.

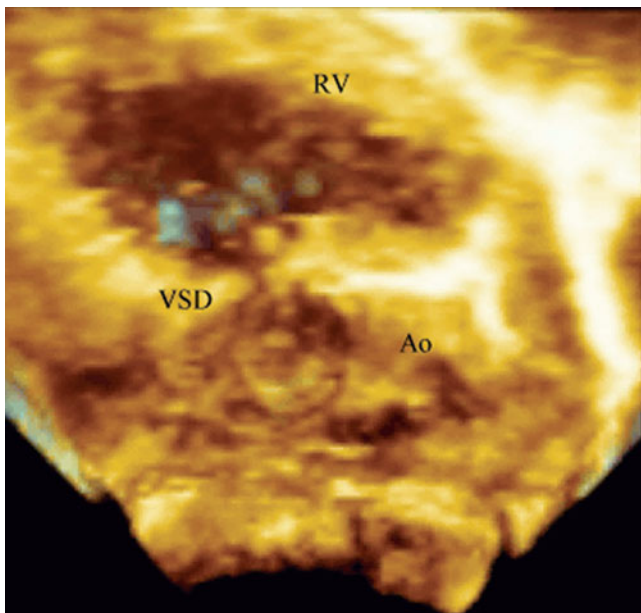


Fig. 19.14 *En face* view of large membranous ventricular septal defect from the left ventricle. *Ao* aorta, *RV* right ventricle, *VSD* ventricular septal defect

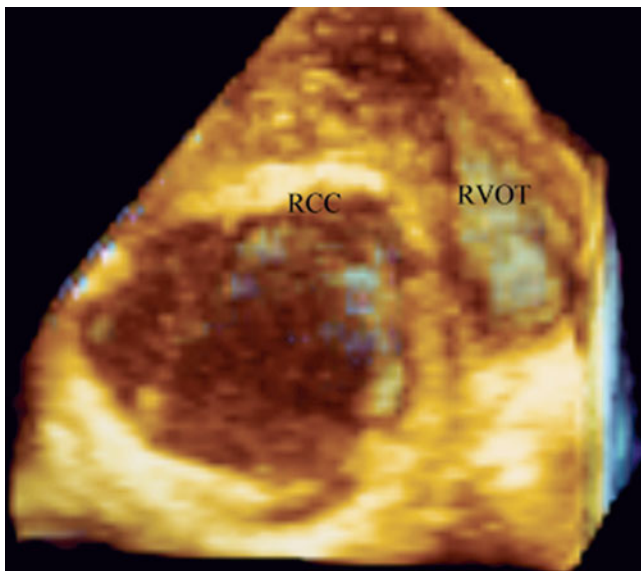


Fig. 19.15 Cross sectional view of doubly committed subarterial ventricular septal defect with prolapse of the right coronary cusp through the defect causing right ventricular outflow tract obstruction. *RCC* right coronary cusp, *RVOT* right ventricular outflow tract

Evaluation of Other Congenital Cardiac Defects

Another conundrum in CHD is complex sub-aortic stenosis. The anatomic substrate is often difficult to define and delineate from associated aortic valve disease. Moreover, an important incidence of re-operation for sub-aortic stenosis persists [79, 80]. Much of this difficulty certainly seems to be related to less than optimal understanding of this complex

anatomy from standard 2D imaging planes. Again, 3D TEE can image the sub-aortic obstruction, in a plane from the LV apex towards the aortic valve (Fig. 19.16, Video 19.12). This view is unavailable to the surgeons unless a left ventriculotomy is performed. The concentric nature of the obstruction, as well as the juxtaposition to the mitral and aortic valve and ventricular septum can be better appreciated in a 3D domain. In older adolescents and young adults who have undergone a myriad of prior surgeries, standard transthoracic imaging may not provide information of sufficient quality to help guide surgical management (due to larger patient size, poorer transthoracic imaging windows, etc.). In such situations, 3D TEE can be employed either as an outpatient procedure, or in the intraoperative setting (before cardiopulmonary bypass) to assist in surgical planning and enhance the success of the surgical intervention [81, 82].

The application of 3D TEE to other congenital cardiac defects is still being developed. A number of case reports have described the use of this modality for evaluation of cor triatriatum [83], aortico LV tunnel [38], corrected and uncorrected transposition of the great arteries [84], and postoperative Fontan [39]. Most of these studies were performed in adult patients with CHD. Interestingly, however, all patients in the Fontan study were 7 years of age or less, underlining the growing use of 3D TEE in the pediatric population.

Further Applications and Development of 3D TEE

The introduction in 2007 of the first commercially available 3D TEE probe (Philips X7-2t 3D TEE probe), along with the large probe size, have limited its widespread applicability in the pediatric population. Nonetheless as discussed above, the published applications of 3D TEE for CHD have steadily grown, both for use in the operating room and interventional catheterization laboratory, as well as a separate diagnostic modality by itself [4, 26–30, 37, 39, 66, 85–87]. In adults, impressive work has already been performed that explores and extends the use of 3D TEE in a number of settings, including those pertinent to adult CHD patients. This includes its use during cardiac surgery [86, 87] and adult transcatheter procedures, along with diagnostic evaluation of atrioventricular and semilunar valve anatomic pathology [15, 20, 86, 88]. Similar to the pediatric population, 3D TEE is used in adults to guide closure of atrial and ventricular septal defects [11, 28, 69, 70, 85]. In addition 3D TEE has proven integral to a number of transcatheter interventional procedures specific to adult cardiology patients including the following: percutaneous mitral valve edge to edge clip technique [11, 89], mitral balloon valvuloplasty [85], left atrial appendage obliteration [90, 91], transcatheter aortic valve implantation (TAVI) [11, 85, 92], and occlu-

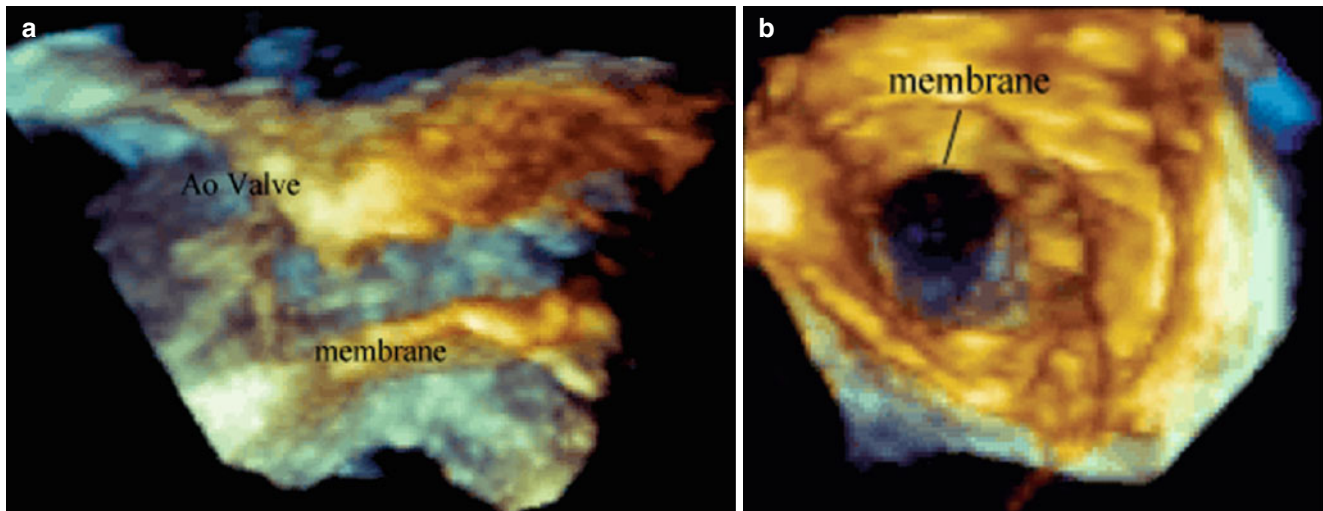


Fig. 19.16 A 7 year old male with severe sub-aortic stenosis. (a) Is a slightly oblique long axis view showing the thickened sub-aortic membrane immediately below the aortic valve. (b) Is a short axis view oriented

from the left ventricular apex to the aorta, and viewed from the left ventricular perspective, demonstrating the concentric nature of the sub-aortic membrane and corresponding small outflow area. *Ao Valve* aortic valve

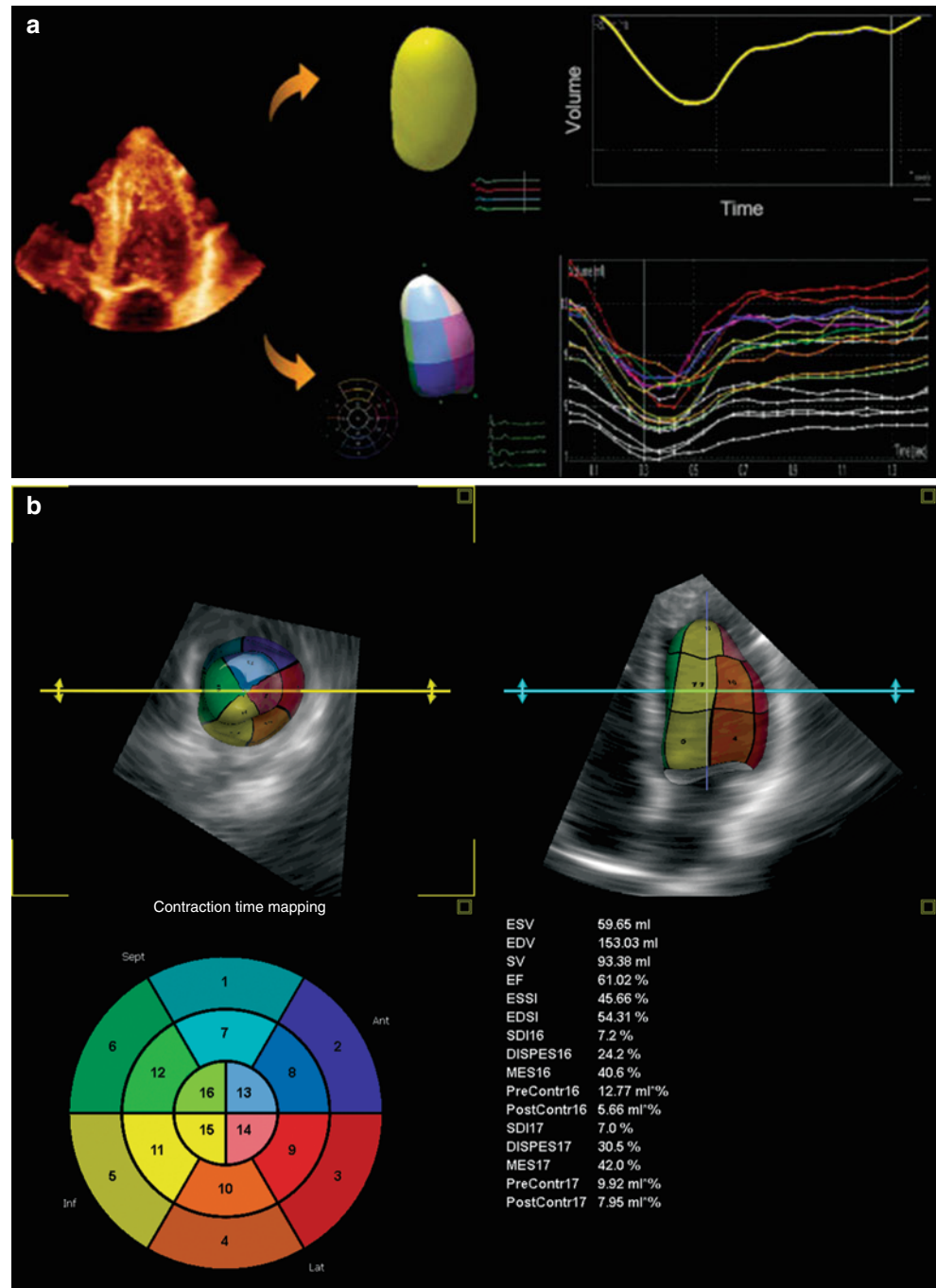
sion of mitral valve perivalvar leaks [11, 21, 93]. The list of these applications is likely to grow significantly in the near future.

There is considerable potential for the use of 3D TEE in the quantitative analysis of cardiac anatomy, mechanics and function. Similar to cardiac magnetic resonance imaging (CMR), the use of a 3D dataset enables volumetric analysis that avoids the geometric assumptions used with 2D methods such as Simpson's method of LV volume calculation. To date, most studies evaluating the assessment of left and right ventricular volumes have been performed using transthoracic 3D echocardiography, and have shown promising results. For the left ventricle, a surface rendered cast chamber is obtained generally by semi-automated border detection of the LV endocardial-blood interface, although manual tracing is sometimes used. The volume is then calculated by direct voxel count and followed throughout the cardiac cycle (Fig. 19.17, Video 19.13). The volumes obtained by 3D echocardiography have been shown to correlate well with CMR, although 3D echocardiography tends to underestimate LV volumes, probably due to its inability to distinguish the trabeculations from myocardium [94–96]. Nonetheless, 3D echocardiographic-measured volumes have better reproducibility than 2D echocardiography [94], and therefore would appear to be a better alternative for the volumetric assessment of the LV. Assessment of RV volumes/function can also be performed by generation of a surface-rendered cast of the RV, usually by semiautomated border quantification using specialized offline software (TomTec 4D echo analysis software, Tom Tec Imaging Systems GmbH, Munich, Germany) (Fig. 19.18, Video 19.14). This analysis can be more involved because of the unusual geometry and shape

of the RV. Using this method, published studies have shown a good correlation between 3D echocardiography and CMR with respect to RV volumes and function [97–99]. However like the 3D evaluation of LV, there appears to be an underestimation of RV volume by 3D echocardiography compared to CMR [100]. Studies evaluating 3D TEE assessment of LV and RV volumes have yet to be performed extensively with 3D TEE [15], but it seems likely that similar results can be obtained with this modality as well. In fact, the superior imaging quality of TEE might actually enhance volume and function assessment in larger patients. Several recent studies have demonstrated the ability of intraoperative 3D TEE to obtain adequate images for subsequent offline measurement of LV/RV volume and function, using images obtained from the mid esophageal window and the same methods of semi-automated border detection [101, 102].

Even more sophisticated evaluations of cardiac mechanics and function have been reported in adults with the use of 3D echocardiography. These evaluations are valuable because they can be difficult to obtain by 2D methods. 3D echocardiography has been shown to be useful for evaluation of LV segmental wall motion analysis and dyssynchrony (Fig. 19.19). Using either a 16 segment model (American Society of Echocardiography) or 17 segment model (American Heart Association) [103], a systolic dyssynchrony index (SDI) can be calculated as the standard deviation of the time required to reach minimum systolic volume for each segment as a percentage of the cardiac cycle (Fig. 19.17b). For normal subjects, the mean SDI (16 segment model) is $3.5 \pm 1.8\%$ [104]. This 3D model of dyssynchrony can be used as one of the measures to evaluate the results of cardiac resynchronization therapy [105–110].

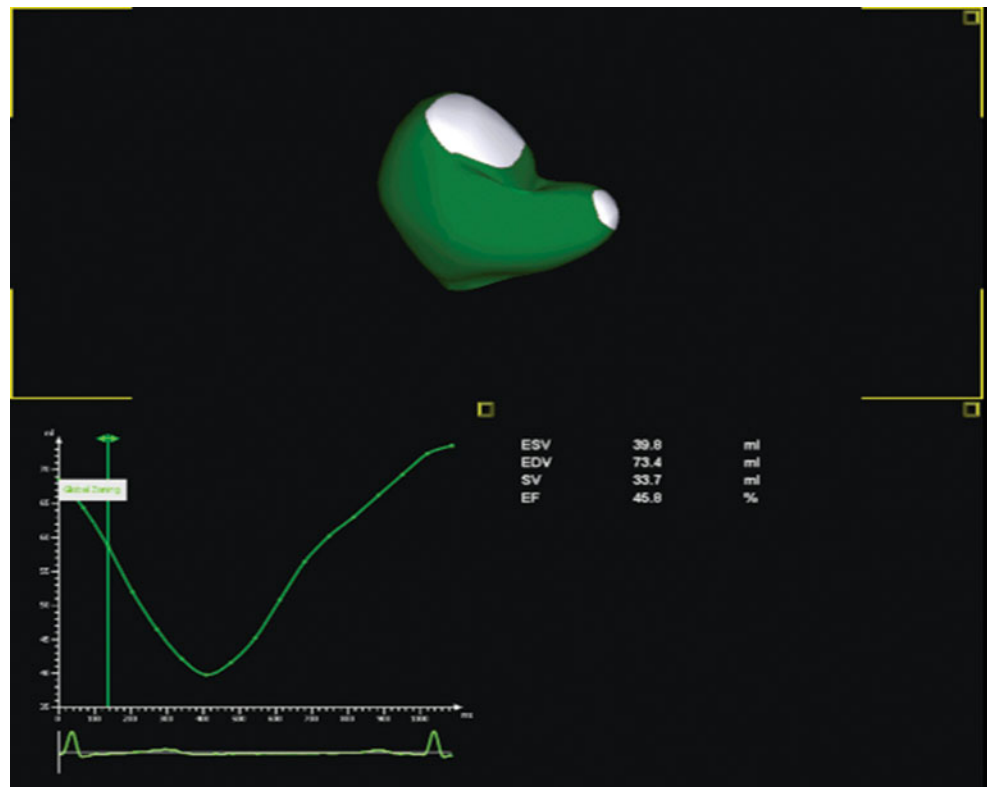
Fig. 19.17 Quantitative assessment of left ventricle (LV) volume and systolic function using three-dimensional (3D) echocardiography. **(a)** From a transthoracic 3D echocardiographic data set of the LV (*left panel*), the LV endocardium can be traced (*middle panel, top*) to obtain the LV volume throughout the cardiac cycle (*right panel, top*). Using the maximum and minimum volumes obtained from this curve, an ejection fraction can be calculated. As well, the LV endocardium can be divided according to the 17-segment mode 1 (*middle panel, bottom*), and the time each segment requires to attain minimal volume in the cardiac cycle can be identified (*right panel, bottom*) (Reprinted from Lang et al. [18]; with permission from Elsevier). **(b)** Evaluation of LV systolic function and dyssynchrony. The upper left and right panels show the 3D surface-rendered LV volume from two views. The *bottom left panel* shows an example of the 16 segment model. Calculation of systolic dyssynchrony index (SDI) can automatically be performed using the 16 segment (SDI 16) and 17 segment (SDI 17) models (*bottom right panel*). See text for details



Several 3D echocardiographic systems provide the ability for offline calculation of myocardial strain, strain rate, rotation, torsion and twist, and some preliminary studies in adults (using transthoracic 3D echocardiography) have already been published that evaluate these parameters [111–114]. Using readily available offline 3D software, quantitative assessment of linear and area measurements can be performed on 3D transthoracic and TEE datasets, along with detailed mitral and aortic valve analysis. The latter allows

for evaluation of noncircular vena contracta (Fig. 19.20) [115] and planimetry of anatomic regurgitant orifice area in mitral regurgitation stenotic orifice area in mitral stenosis [116, 117]. Recently, 3D TEE has enabled sophisticated evaluation of mitral valve parametric mapping [118] and volumetric quantification (Fig. 19.21) [18], aortic valve dynamic motion (Fig. 19.22) [18, 22], and mitral-aortic valve coupling [119]. An important disadvantage of most of the aforementioned analyses (including volume/function

Fig. 19.18 Quantitative assessment of right ventricular (RV) volume and systolic function using three-dimensional (3D) echocardiography, using software from TomTec (4D RV-function®). From a full volume transthoracic 3D echocardiographic data set of the RV, the endocardium is manually traced in three orthogonal planes. The software utilizes a semi-automated border detection method to generate a dynamic model of the RV, which is displayed in the *top panel*. RV volume is displayed on a curve of volume over time throughout the cardiac cycle in the *lower left panel*. The RV stroke volume (SV) and ejection fraction (EF) are automatically calculated and displayed in the *lower right panel*



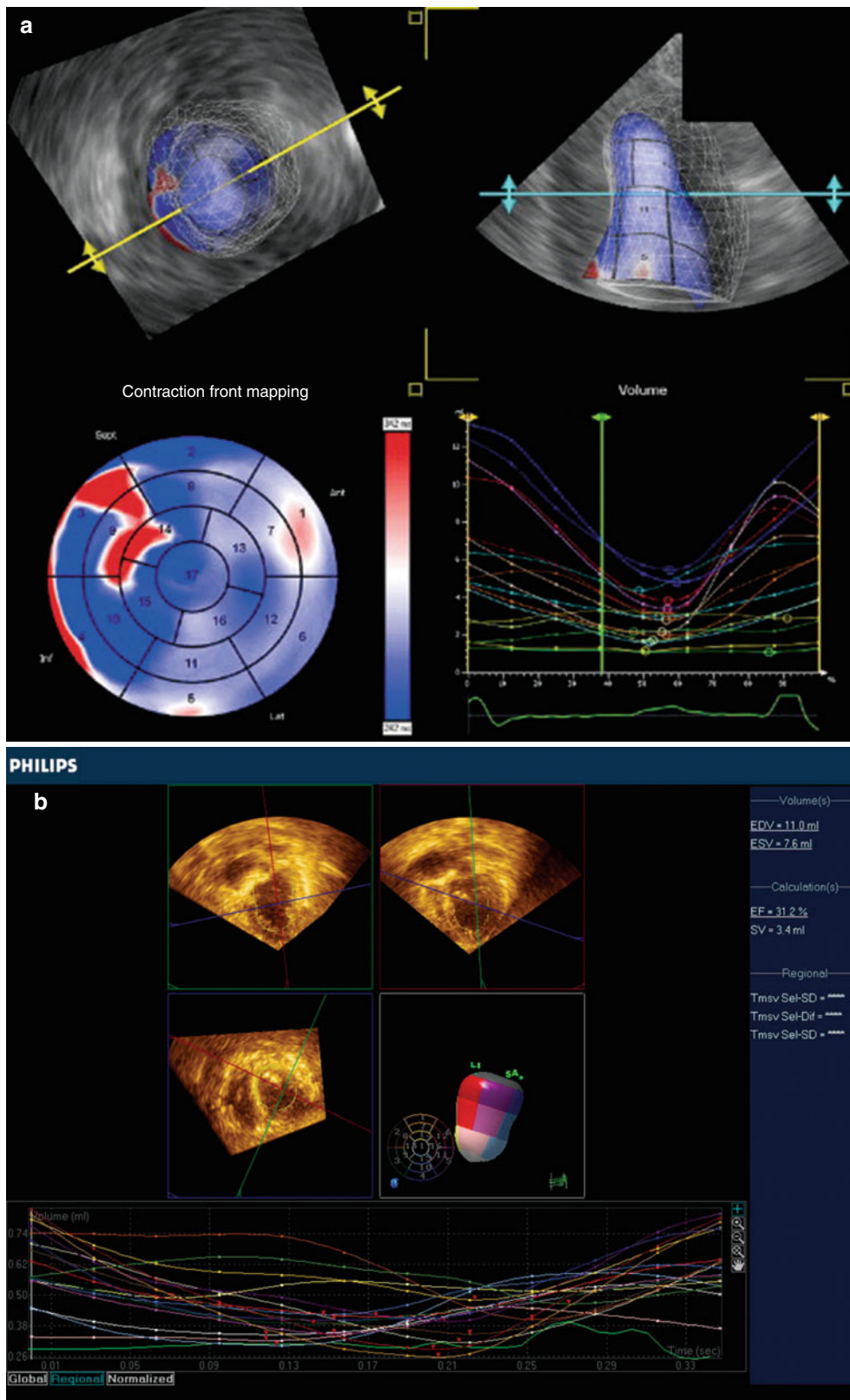
quantification) is that they must be performed offline and the analysis can be rather time-consuming, thus limiting their immediate utility in the intraoperative and interventional cardiology settings where rapid access to information is essential [120]. However 3D echocardiography systems are rapidly evolving, and future advances in semi-automated quantification, as well as on-cart availability of analysis tools, could make many of the quantitative 3D TEE analyses readily accessible at the time of the study. One previous report of 3D TEE during a Ross procedure demonstrated the use of 3D volumetric and function quantification before and after cardiopulmonary bypass (using techniques described above); the authors were able to quantify LV function and identify wall motion abnormalities following bypass [53]. A 3–5 min time period was needed for quantification, and this short period of time allowed it to be performed contemporaneously with the operation.

The other important consideration pertains to the use of 3D TEE for quantitative analysis of cardiac mechanics and function in patients with CHD. The evaluations of right and single ventricle volumes and function are currently some of the most important and active areas of investigation among CHD specialists. These type of evaluations are pertinent for a number of important and topical issues in CHD: RV function in postoperative tetralogy of Fallot patients with chronic pulmonary regurgitation, ventricular function in various forms of single ventricle/Fontan patients, function of the systemic RV in congenitally corrected transposition of the great arteries, and other clinically challenging conditions.

Currently CMR is the gold standard for quantification of ventricular volumes and function in these settings, but a number of pediatric studies have shown a reasonably good correlation between 3D echocardiography and CMR in volumes and function for the LV [121–126], RV [99, 101, 127–129], and even single ventricles [130, 131]. These studies were performed primarily with transthoracic 3D echocardiography, and it remains to be seen how useful and effective 3D TEE will be in this setting. This represents one of the many interesting areas of future research in 3D echocardiography.

Another interesting area for future development is the use of 3D color flow Doppler (3D CFD) for evaluation of CHD. As noted earlier in this chapter, 3D CFD is used qualitatively for assessment of atrioventricular and semilunar valve pathology, to localize and display sites of stenosis or regurgitation. In addition, 3D CFD has been utilized in CHD as an “echocardiographic angiogram” to assess vascular structures such as coarctation, vascular ring, and systemic to pulmonary artery shunts [132]. Quantitative use of 3D CFD also holds some promise as a method of volumetric flow assessment [133]. A recent study by Poh et al. evaluated cardiac output in sheep with experimentally distorted ventricular septal geometry, and found that, using flow-probe data as a reference standard, a much better correlation was obtained when calculated by 3D CFD as compared to 2D-derived methods [134]. Lu et al. have compared the use of 3D CFD to 3D ventricular volumetric calculations as a method for measurement of valvar volumetric flow in children. These

Fig. 19.19 Evaluation of left ventricle (LV) segmental wall motion. (a) Shows a three-dimensional transthoracic echocardiogram data set of the LV as viewed from the apex (*left, top*) or anteriorly (*right, top*), with dynamic tracking of the LV endocardium. The end-diastolic LV endocardium is visualized as a mesh shell and the end-systolic endocardium as a solid shell. *Lower left*: a 17-segment, bull’s-eye map of contraction front mapping demonstrating the time required for each segment to reach minimal LV volume (*left, bottom*). *Lower right*: Graph, with time along the x axis and volume along the y axis, demonstrating the time for each segment to reach minimal volume. *Ant* anterior, *Inf* inferior, *Lat* lateral, *Sept* septum (Reprinted from Lang et al. [18]; with permission from Elsevier). (b) Is taken from a patient with dilated cardiomyopathy and dyssynchronous LV contraction; note the marked lack of synchrony of the individual cardiac segments as compared to Fig. 19.17a



investigators found the best correlation with the mitral valve, good correlations for aortic and pulmonary valves, and a poor correlation with the tricuspid valve [135]. Nonetheless despite the encouraging data from these studies, more

investigation will need to be performed to verify the utility of 3D CFD, especially given the potentially limiting factors of smaller volume datasets, stitch artifact, and marginal spatial/temporal resolution. Improvements in 3D CFD technology,

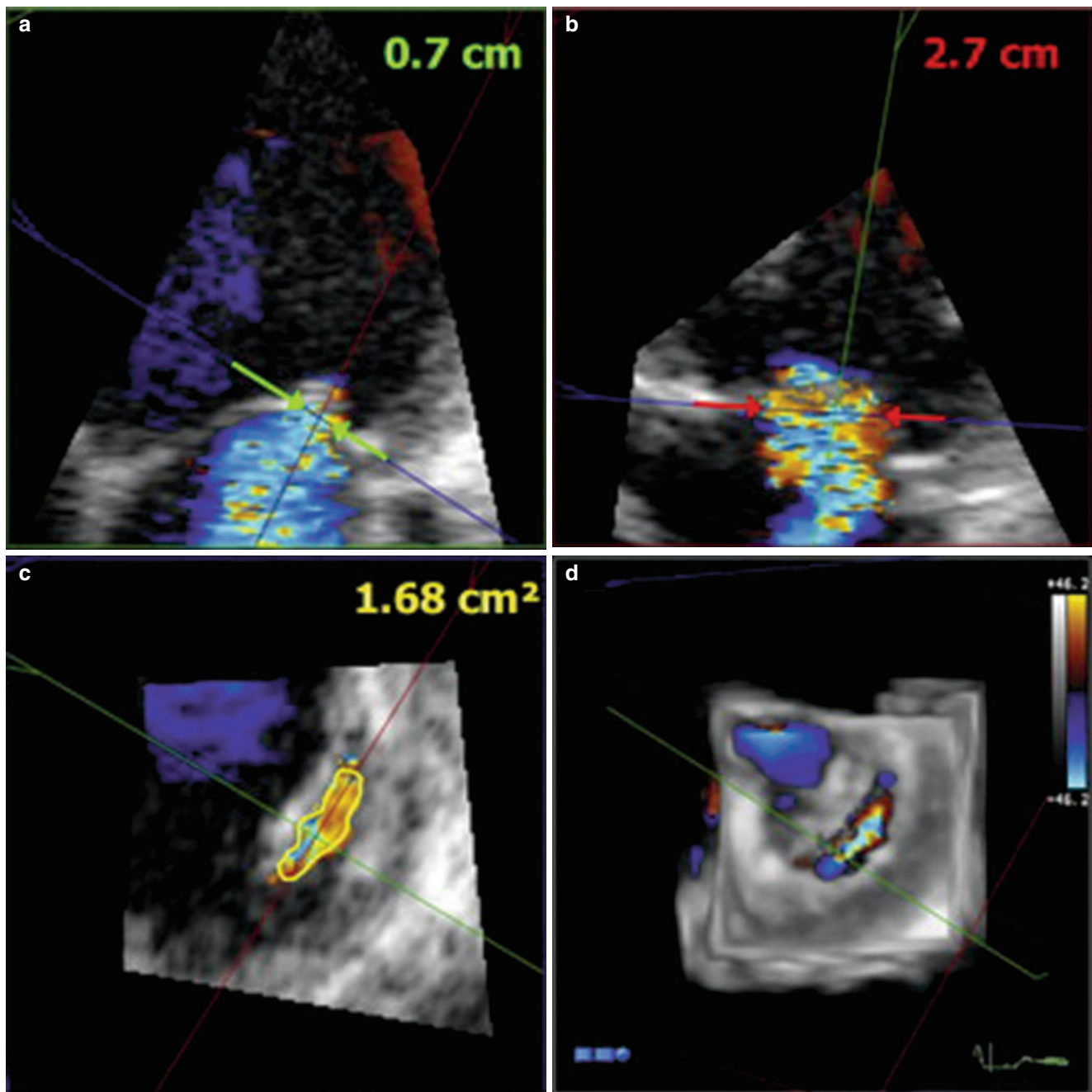


Fig. 19.20 Example of measurement of vena contracta (VC) dimensions in a cross-sectional plane through the VC in a patient with functional mitral regurgitation caused by leaflet tethering. Panel **a** shows a four-chamber view with measurement of a narrow VC width. Panel **b** shows a two chamber view with measurement of a broad VC width. Panel **c** shows a cross-sectional plane through the VC with direct pla-

nimetry of vena contracta area. The *green* and the *red* lines indicate the orientation of the four chamber plane (panel **a**, *green* frame) and the two chamber plane (panel **b**, *red* frame). Panel **d** shows a 3D *en face* view of VC area. Note that the significant asymmetry of the VC area makes difficult the accurate assessment of regurgitation from a single plane (From Kahlert et al. [115]; with permission from Elsevier)

along with more robust semi-automated flow quantification tools, will likely enhance the utility of these techniques [43].

Until recently, the availability of 3D TEE from only one company also provided some limitation, as it was necessary for practitioners to purchase or already own the echocardiographic system that accommodated this probe. However,

another 3D TEE probe is now commercially available from a second major company (BT-12 3D/4D TEE probe, GE Medical Systems), and it is anticipated that other companies will follow. This should stimulate further adoption of 3D TEE in a number of clinical settings, including that of CHD evaluation.

3D Imaging: Limitations, Artifacts, and Pitfalls

Despite its growing popularity, 3D imaging still has important potential limitations with which the examiner should be aware. First, despite the dramatic advances in 3D technology, both spatial and temporal resolutions are still inferior to that of comparable 2D imaging. The 3D TEE probe images at the same high frequency (7 MHz) as many adult TEE probes as well as some pediatric transthoracic probes, but some degree of fine gray scale and tissue detail are lost when imaging in 3D. Temporal resolution is also reduced (sometimes significantly) when compared to 2D imaging, and this can impair the ability to visualize precise motion of structures such as atrioventricular and semilunar valves. It can also be a potential issue in younger patients with faster heart rates; the lower frame rates can result in cardiac motion that appears less smooth.

Since 3D echocardiography is still a form of ultrasound, it will be subject to the same artifacts as those encountered with 2D echocardiography, such as reverberations and shadowing. In addition, there are some artifacts particular to 3D imaging. Such artifacts include false dropout of certain areas due to lack of 3D data collected by the matrix transducer. This can also occur because of reduced gain settings that lead to data loss. The result is transparency or apparent absence of tissue in certain structures such as the atrioventricular and semilunar valves. In some cases, the dropout can mimic an anatomic defect. It

can also become apparent when nonstandard cropping planes are used, due to the data loss that can occur from objects oriented more parallel to the ultrasound beam(s) [136]. To compensate, gain settings can be increased but too much gain will lead to speckling artifacts and worsened 3D rendering that can obscure cardiac structures. Another important artifact is the “stitch artifact” (described above) that can occur with full volume imaging, due to irregularities in ECG gating and/or movement of the cardiac position from respiration or other external factors (Fig. 19.23, Video 19.15). This can introduce errors in the depiction of real-time motion [18].

The other important point is that the 3D images actually represent 2D renderings of 3D structures, with color shading used to give the perception of depth. While 3D TEE images provide excellent detail, it can be difficult to determine the precise front to back spatial orientation of cardiac structures in a given 3D image. These 3D relationships can be particularly important with CHD. Thus it is important to perform both cropping and rotation of a 3D rendering, and to visualize a cardiac structure in several different views [18].

Summary

3D TEE has become an integral part in the evaluation of patients with complex CHD at our medical center and other facilities that care for these patients. Such imaging provides

Fig. 19.21 Quantitative evaluation of the mitral valve. (a) Volumetric quantification of the mitral valve allows accurate measurements of the height of the saddle-shaped mitral valve (*top left*), commissure-to-commissure diameter measurements of the mitral annulus (*bottom left*), mitral annular surface area (*top right*), and the angle between the aortic root and the mitral annulus (*bottom right*). A Anterior, AL anterolateral, Ao aorta, P posterior, PM posteromedial (Reprinted from Lang et al. [18]; with permission from Elsevier). (b) Mitral valve evaluation using TomTec 4D MV-Assessment© software. *Top panel* shows dynamic 3D depiction of mitral valve P2 scallop prolapse. *Bottom panel* shows various quantitative measurements available for mitral valve assessment. (Reprinted with permission of TomTec Imaging Systems GmbH, Munich, Germany)

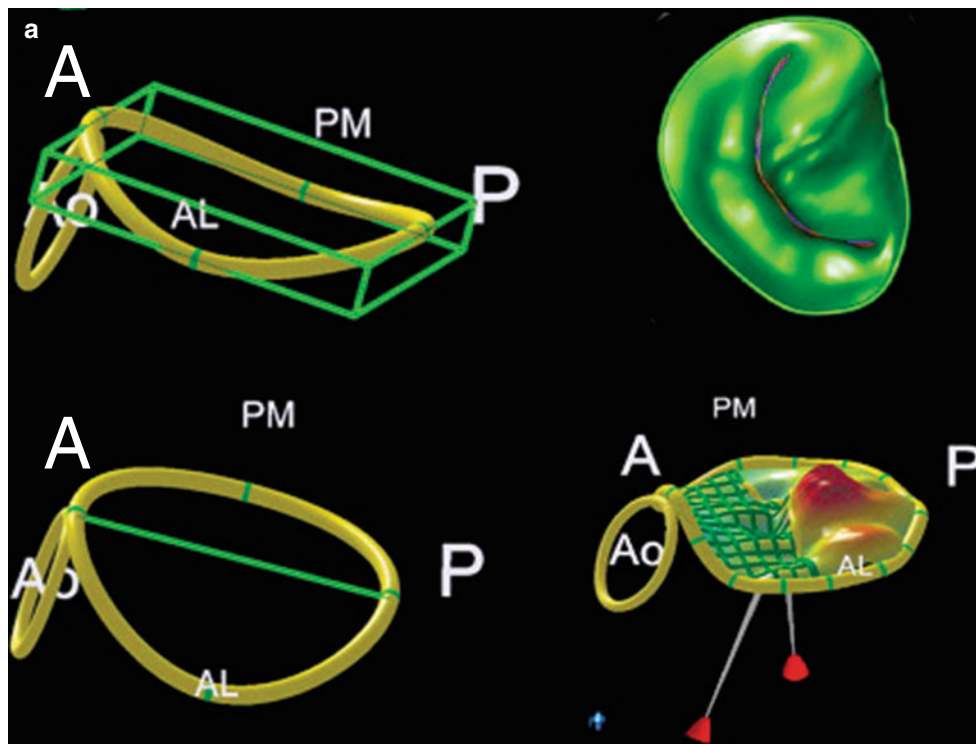
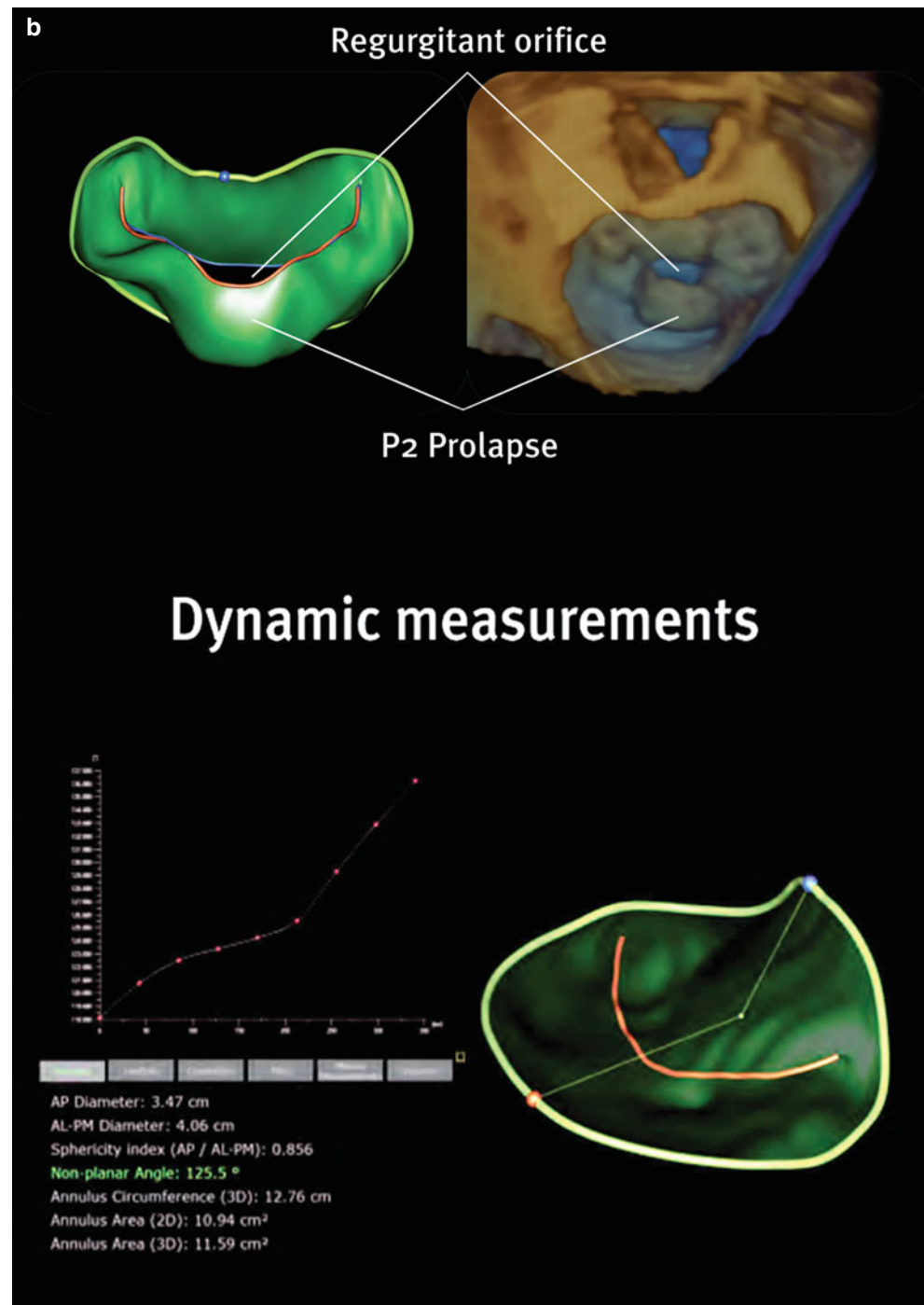


Fig. 19.21 (continued)



unique planes and projections that are unavailable with standard 2D display. Moreover, in pre and post bypass patients the heart and corresponding anatomy is depicted in dynamic motion, rather than the surgeon's perspective of the non-beating heart.

Certain aspects will need to continue to evolve, for example improved imaging in the near field is necessary. Transesophageal probes need to be reduced in size, with higher transmit frequencies for the smaller pediatric patients.

Live full volume imaging will be more advantageous with improved temporal resolution (for the faster heart rates in children) and overall improved spatial resolution. Also, the ability to perform online linear, area and volume measurements directly on the echocardiography machine will facilitate the ability to provide timely important information to surgeons and interventional cardiologists. This will be further enhanced by automated quantification tools that are beginning to appear on the advanced 3D echocardiography platforms.

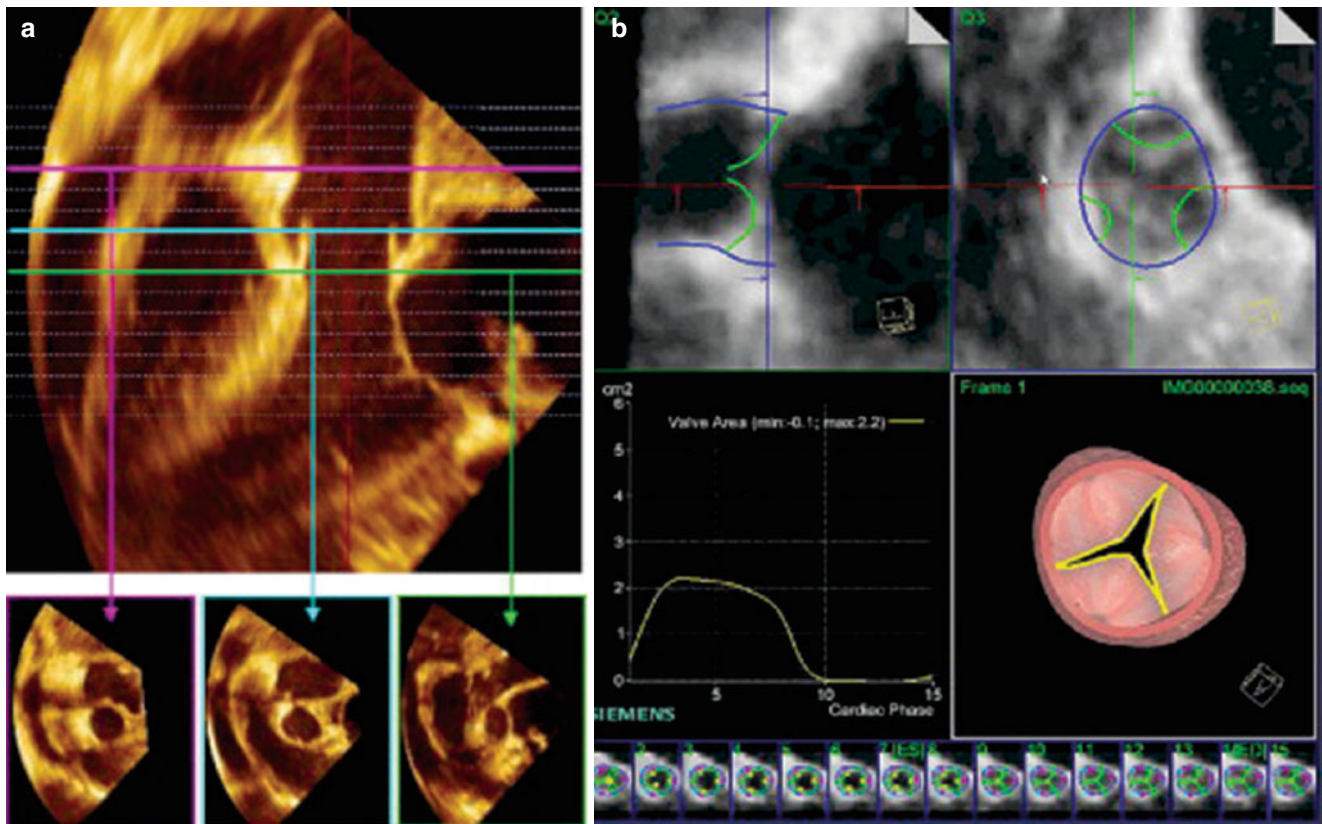


Fig. 19.22 Three-dimensional transesophageal data set cropped to demonstrate the aorta in long axis (**a**, *top*). Using this image, *en face* views of the sinotubular junction (**a**, *bottom left*), sinus of Valsalva (**a**, *bottom middle*), and aortic annulus (**a**, *bottom right*) can be obtained for assessment. Dynamic, automatic tracking of the aortic valve leaflets (**b**,

top left) and annulus (**b**, *top right*) can be performed, providing aortic valve area throughout the cardiac cycle (**b**, *middle left* and *bottom strip*). A model derived from the automated tracking is also produced (*middle right*) (Reprinted from Lang et al. [18]; with permission from Elsevier)

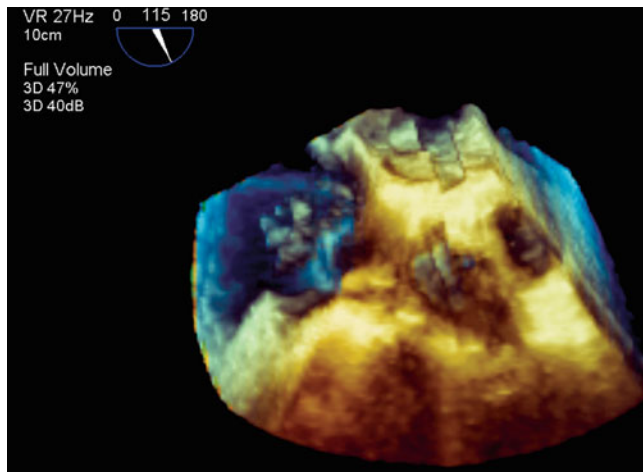


Fig. 19.23 Example of stitch artifact with a full volume dataset. This can occur as a result of irregularities in cardiac rhythm, or respiratory/patient movement

Equally important for successful development of 3D TEE imaging are the interactions between the cardiologist and surgeon in trying to comprehend and display this complex

anatomy. Intraoperative 3D TEE imaging is still early in development, and cooperation between surgeons, anesthesiologists, and cardiologists will hasten this progress.

References

1. Belohlavek M, Foley DA, Gerber TC, Greenleaf JF, Seward JB. Three-dimensional ultrasound imaging of the atrial septum: normal and pathologic anatomy. *J Am Coll Cardiol.* 1993;22:1673–8.
2. Marx GR, Fulton DR, Pandian NG, et al. Delineation of site, relative size and dynamic geometry of atrial septal defects by real-time three-dimensional echocardiography. *J Am Coll Cardiol.* 1995;25:482–90.
3. Franke A, Kühn HP, Rulands D, et al. Quantitative analysis of the morphology of secundum-type atrial septal defects and their dynamic change using transesophageal three-dimensional echocardiography. *Circulation.* 1997;96:II-323-7.
4. Cao Q, Radtke W, Berger F, Zhu W, Hijazi ZM. Transcatheter closure of multiple atrial septal defects. Initial results and value of two- and three-dimensional transesophageal echocardiography. *Eur Heart J.* 2000;21:941–7.
5. Mumm B, Nanda NC, Sorrell VL, et al. Technical background and current & future aspects of three-dimensional echocardiography. In: Nanda NC, Sorrell VL, editors. *Atlas of three-dimensional*

- echocardiography. Armonk: Futura Publishing Company, Inc.; 2002. p. 1–20.
6. Miller AP, Nanda NC, Aaluri S, et al. Three-dimensional transesophageal echocardiographic demonstration of anatomical defects in AV septal defect patients presenting for reoperation. *Echocardiography*. 2003;20:105–9.
 7. Vida VL, Hoehn R, Larrazabal LA, Gauvreau K, Marx GR, del Nido PJ. Usefulness of intra-operative epicardial three-dimensional echocardiography to guide aortic valve repair in children. *Am J Cardiol*. 2009;103:852–6.
 8. Salandin V, De Castro S, Cavarretta E, et al. Epicardial real-time 3-dimensional echocardiography with the use of a pediatric transthoracic probe: a technical approach. *J Cardiothorac Vasc Anesth*. 2010;24:43–50.
 9. Sugeng L, Shernan SK, Salgo IS, et al. Live 3-dimensional transesophageal echocardiography initial experience using the fully-sampled matrix array probe. *J Am Coll Cardiol*. 2008;52:446–9.
 10. Sugeng L, Weinert L, Lang RM. Left ventricular assessment using real time three dimensional echocardiography. *Heart*. 2003;89 Suppl 3:iii29–36.
 11. Perk G, Lang RM, Garcia-Fernandez MA, et al. Use of real time three-dimensional transesophageal echocardiography in intracardiac catheter based interventions. *J Am Soc Echocardiogr*. 2009;22:865–82.
 12. Mackensen GB, Swaminathan M, Mathew JP. PRO editorial: PRO: three-dimensional transesophageal echocardiography is a major advance for intraoperative clinical management of patients undergoing cardiac surgery. *Anesth Analg*. 2010;110:1574–8.
 13. Baker GH, Shirali G, Ringewald JM, Hsia TY, Bandisode V. Usefulness of live three-dimensional transesophageal echocardiography in a congenital heart disease center. *Am J Cardiol*. 2009;103:1025–8.
 14. Salgo IS. Three-dimensional echocardiographic technology. *Cardiol Clin*. 2007;25:231–9.
 15. Vegas A, Meineri M. Core review: three-dimensional transesophageal echocardiography is a major advance for intraoperative clinical management of patients undergoing cardiac surgery: a core review. *Anesth Analg*. 2010;110:1548–73.
 16. Salgo IS. 3D transesophageal echocardiographic technologies. In: Badano LP, Lang RM, Zamorano JL, editors. *Textbook of real-time three dimensional echocardiography*. London: Springer; 2011. p. 25–32.
 17. Rabben SI. Technical principles of transthoracic three-dimensional echocardiography. In: Badano LP, Lang RM, Zamorano JL, editors. *Textbook of real-time three dimensional echocardiography*. London: Springer; 2011. p. 9–24.
 18. Lang RM, Badano LP, Tsang W, et al. EAE/ASE recommendations for image acquisition and display using three-dimensional echocardiography. *J Am Soc Echocardiogr*. 2012;25:3–46.
 19. Bharucha T, Roman KS, Anderson RH, Vettukattil JJ. Impact of multiplanar review of three-dimensional echocardiographic data on management of congenital heart disease. *Ann Thorac Surg*. 2008;86:875–81.
 20. Grewal J, Mankad S, Freeman WK, et al. Real-time three-dimensional transesophageal echocardiography in the intraoperative assessment of mitral valve disease. *J Am Soc Echocardiogr*. 2009;22:34–41.
 21. Kronzon I, Sugeng L, Perk G, et al. Real-time 3-dimensional transesophageal echocardiography in the evaluation of post-operative mitral annuloplasty ring and prosthetic valve dehiscence. *J Am Coll Cardiol*. 2009;53:1543–7.
 22. Mahmood F, Subramaniam B, Gorman JH, et al. Three-dimensional echocardiographic assessment of changes in mitral valve geometry after valve repair. *Ann Thorac Surg*. 2009;88:1838–44.
 23. Scohy TV, Soliman OII, Lecomte PVEL, et al. Intraoperative real time three-dimensional transesophageal echocardiographic measurement of hemodynamic, anatomic and functional changes after aortic valve replacement. *Echocardiography*. 2009;26:96–9.
 24. Kelpis TG, Ninios VN, Dardas PS, Pitsis AA. Subaortic stenosis in an adult caused by two discrete membranes: a three-dimensional transesophageal echocardiographic visualization. *Ann Thorac Surg*. 2009;88:1703.
 25. van Noord PT, Scohy TV, McGhie J, Bogers AJJC. Three-dimensional transesophageal echocardiography in Ebstein's anomaly. *Interact Cardiovasc Thorac Surg*. 2010;10:836–7.
 26. Acar P, Dulac Y, Roux D, Rougé P, Duterque D, Aggoun Y. Comparison of transthoracic and transesophageal three-dimensional echocardiography for assessment of atrial septal defect diameter in children. *Am J Cardiol*. 2003;91:500–2.
 27. Georgakis A, Radtke WAK, Lopez C, et al. Complex atrial septal defect: percutaneous repair guided by three-dimensional echocardiography. *Echocardiography*. 2010;27:590–3.
 28. Price MJ, Smith MR, Rubenson DS. Utility of on-line three-dimensional transesophageal echocardiography during percutaneous atrial septal defect closure. *Catheter Cardiovasc Interv*. 2010;75:570–7.
 29. Saric M, Perk G, Purgess JR, Kronzon I. Imaging atrial septal defects by real-time three-dimensional transesophageal echocardiography: step-by-step approach. *J Am Soc Echocardiogr*. 2010;23:1128–35.
 30. Dall'Agata A, Cromme-Dijkhuis AH, Meijboom FJ, et al. Use of three-dimensional echocardiography for analysis of outflow obstruction in congenital heart disease. *Am J Cardiol*. 1999;83:921–5.
 31. Chan K-L, Liu X, Ascah KJ, Beauchesne LM, Burwash IG. Comparison of real-time 3-dimensional echocardiography with conventional 2-dimensional echocardiography in the assessment of structural heart disease. *J Am Soc Echocardiogr*. 2004;17:976–80.
 32. Takahashi K, Mackie AS, Rebeyka IM, et al. Two-dimensional versus transthoracic real-time three-dimensional echocardiography in the evaluation of the mechanisms and sites of atrioventricular valve regurgitation in a congenital heart disease population. *J Am Soc Echocardiogr*. 2010;23:726–34.
 33. Simpson JM, Miller O. Three-dimensional echocardiography in congenital heart disease. *Arch Cardiovasc Dis*. 2011;104:45–56.
 34. Yagel S, Cohen SM, Rosenak D, et al. Added value of three-/four-dimensional ultrasound in offline analysis and diagnosis of congenital heart disease. *Ultrasound Obstet Gynecol*. 2011;37:432–7.
 35. Shirali GS. Three-dimensional echocardiography in congenital heart disease. *Echocardiography*. 2012;29:242–8.
 36. Vettukattil JJ. Three dimensional echocardiography in congenital heart disease. *Heart*. 2012;98:79–88.
 37. Magni G, Hijazi ZM, Pandian NG, et al. Two- and three-dimensional transesophageal echocardiography in patient selection and assessment of atrial septal defect closure by the new DAS-Angel Wings device: initial clinical experience. *Circulation*. 1997;96:1722–8.
 38. Chang C-Y, Hsiung MC, Tsai SK, et al. Live three-dimensional transesophageal echocardiography in an unusual case of aorto-left ventricular tunnel with a large interventricular septal aneurysm. *Echocardiography*. 2011;28:E12–5.
 39. Mart CR. Three-dimensional echocardiographic evaluation of the Fontan conduit for thrombus. *Echocardiography*. 2012;29:363–8.
 40. Salcedo EE, Quaipe RA, Seres T, Carroll JD. A framework for systematic characterization of the mitral valve by real-time three-dimensional transesophageal echocardiography. *J Am Soc Echocardiogr*. 2009;22:1087–99.

41. Lang RM, Tsang W, Weinert L, Mor-Avi V, Chandra S. Valvular heart disease the value of 3-dimensional echocardiography. *J Am Coll Cardiol.* 2011;58:1933–44.
42. Vettukattil JJ, Bharucha T, Anderson RH. Defining Ebstein's malformation using three-dimensional echocardiography. *Interact Cardiovasc Thorac Surg.* 2007;6:685–90.
43. Zhang L, Xie M, Balluz R, Ge S. Real time three-dimensional echocardiography for evaluation of congenital heart defects: state of the art. *Echocardiography.* 2012;29:232–41.
44. Valverde I, Rawlins D, Austin C, Simpson JM. Three-dimensional echocardiography in the management of parachute mitral valve. *Eur Heart J Cardiovasc Imaging.* 2012;13:446.
45. Anwar AM, McGhie JS, Meijboom FJ, Ten Cate FJ. Double orifice mitral valve by real-time three-dimensional echocardiography. *Eur J Echocardiogr.* 2008;9:731–2.
46. Han J, He Y, Li Z, et al. Isolated double-orifice mitral valve anomaly on 3-dimensional transesophageal echocardiography. *J Ultrasound Med.* 2009;28:1589–92.
47. Seliem MA, Fedec A, Szwaast A, et al. Atrioventricular valve morphology and dynamics in congenital heart disease as imaged with real-time 3-dimensional matrix-array echocardiography: comparison with 2-dimensional imaging and surgical findings. *J Am Soc Echocardiogr.* 2007;20:869–76.
48. da Silva JP, Baumgratz JF, da Fonseca L, et al. The cone reconstruction of the tricuspid valve in Ebstein's anomaly. The operation: early and midterm results. *J Thorac Cardiovasc Surg.* 2007;133:215–23.
49. Kiziltan HT, Theodoro DA, Warnes CA, O'Leary PW, Anderson BJ, Danielson GK. Late results of bioprosthetic tricuspid valve replacement in Ebstein's anomaly. *Ann Thorac Surg.* 1998;66:1539–45.
50. Dearani JA, Danielson GK. Surgical management of Ebstein's anomaly in the adult. *Semin Thorac Cardiovasc Surg.* 2005;17:148–54.
51. Sugeng L, Shernan SK, Weinert L, et al. Real-time three-dimensional transesophageal echocardiography in valve disease: comparison with surgical findings and evaluation of prosthetic valves. *J Am Soc Echocardiogr.* 2008;21:1347–54.
52. Kwak J, Andrawes M, Garvin S, D'Ambra MN. 3D transesophageal echocardiography: a review of recent literature 2007–2009. *Curr Opin Anaesthesiol.* 2010;23:80–8.
53. Weitzel N, Salcedo E, Puskas F, Nasrallah F, Fullerton D, Seres T. Using real time three-dimensional transesophageal echocardiography during Ross procedure in the operating room. *Echocardiography.* 2009;26:1278–83.
54. Brantley HP, Nekkanti R, Anderson CA, Kypson AP. Three-dimensional echocardiographic features of unicuspid aortic valve stenosis correlate with surgical findings. *Echocardiography.* 2012;29:E204–7.
55. Bharucha T, Fernandes F, Slorach C, Mertens L, Friedberg MK. Measurement of effective aortic valve area using three-dimensional echocardiography in children undergoing aortic balloon valvuloplasty for aortic stenosis. *Echocardiography.* 2012;29:484–91.
56. Chin C-H, Chen C-H, Lo H-S. The correlation between three-dimensional vena contracta area and aortic regurgitation index in patients with aortic regurgitation. *Echocardiography.* 2010;27:161–6.
57. Khaw AV, Bardeleben RSV, Strasser C, et al. Direct measurement of left ventricular outflow tract by transthoracic real-time 3D-echocardiography increases accuracy in assessment of aortic valve stenosis. *Int J Cardiol.* 2009;136:64–71.
58. Gaspar T, Adawi S, Sachner R, et al. Three-dimensional imaging of the left ventricular outflow tract: impact on aortic valve area estimation by the continuity equation. *J Am Soc Echocardiogr.* 2012;25:749–57.
59. Saitoh T, Shiota M, Izumo M, et al. Comparison of left ventricular outflow geometry and aortic valve area in patients with aortic stenosis by 2-dimensional versus 3-dimensional echocardiography. *Am J Cardiol.* 2012;109:1626–31.
60. Baumgartner H, Hung J, Bermejo J, et al. Echocardiographic assessment of valve stenosis: EAE/ASE recommendations for clinical practice. *J Am Soc Echocardiogr.* 2009;22:1–23; quiz 101–2.
61. Anwar AM, Soliman O, van den Bosch AE, et al. Assessment of pulmonary valve and right ventricular outflow tract with real-time three-dimensional echocardiography. *Int J Cardiovasc Imaging.* 2007;23:167–75.
62. Cheng TO, Xie M-X, Wang X-F, Wang Y, Lu Q. Real-time 3-dimensional echocardiography in assessing atrial and ventricular septal defects: an echocardiographic-surgical correlative study. *Am Heart J.* 2004;148:1091–5.
63. Chen FL, Hsiung MC, Nanda N, Hsieh KS, Chou MC. Real time three-dimensional echocardiography in assessing ventricular septal defects: an echocardiographic-surgical correlative study. *Echocardiography.* 2006;23:562–8.
64. Mercer-Rosa L, Seliem MA, Fedec A, Rome J, Rychik J, Gaynor JW. Illustration of the additional value of real-time 3-dimensional echocardiography to conventional transthoracic and transesophageal 2-dimensional echocardiography in imaging muscular ventricular septal defects: does this have any impact on individual patient treatment? *J Am Soc Echocardiogr.* 2006;19:1511–9.
65. van den Bosch AE, Ten Harkel D-J, McGhie JS, et al. Feasibility and accuracy of real-time 3-dimensional echocardiographic assessment of ventricular septal defects. *J Am Soc Echocardiogr.* 2006;19:7–13.
66. Acar P, Abadir S, Aggoun Y. Transcatheter closure of perimembranous ventricular septal defects with Amplatzer occluder assessed by real-time three-dimensional echocardiography. *Eur J Echocardiogr.* 2007;8:110–5.
67. Huang X, Shen J, Huang Y, et al. En face view of atrial septal defect by two-dimensional transthoracic echocardiography: comparison to real-time three-dimensional transesophageal echocardiography. *J Am Soc Echocardiogr.* 2010;23:714–21.
68. Morgan GJ, Casey F, Craig B, Sands A. Assessing ASDs prior to device closure using 3D echocardiography. Just pretty pictures or a useful clinical tool? *Eur J Echocardiogr.* 2008;9:478–82.
69. Taniguchi M, Akagi T, Watanabe N, et al. Application of real-time three-dimensional transesophageal echocardiography using a matrix array probe for transcatheter closure of atrial septal defect. *J Am Soc Echocardiogr.* 2009;22:1114–20.
70. Halpern DG, Perk G, Ruiz C, Marino N, Kronzon I. Percutaneous closure of a post-myocardial infarction ventricular septal defect guided by real-time three-dimensional echocardiography. *Eur J Echocardiogr.* 2009;10:569–71.
71. Zhu D, Tao K-Y, Liu B. Successful repair of a traumatic ventricular septal defect using an amplatzer occluder guided by three-dimensional transesophageal echocardiography. *J Card Surg.* 2010;25:685–9.
72. Van der Velde ME, Sanders SP, Keane JF, Perry SB, Lock JE. Transesophageal echocardiographic guidance of transcatheter ventricular septal defect closure. *J Am Coll Cardiol.* 1994;23:1660–5.
73. Holzer R, Balzer D, Cao Q-L, Lock K, Hijazi ZM, Amplatzer Muscular Ventricular Septal Defect Investigators. Device closure of muscular ventricular septal defects using the Amplatzer muscular ventricular septal defect occluder: immediate and mid-term results of a U.S. registry. *J Am Coll Cardiol.* 2004;43:1257–63.
74. Bacha EA, Cao QL, Galantowicz ME, et al. Multicenter experience with perventricular device closure of muscular ventricular septal defects. *Pediatr Cardiol.* 2005;26:169–75.

75. Butera G, Chessa M, Carminati M. Percutaneous closure of ventricular septal defects. *Cardiol Young*. 2007;17:243–53.
76. Gan C, An Q, Lin K, et al. Periventricular device closure of ventricular septal defects: six months results in 30 young children. *Ann Thorac Surg*. 2008;86:142–6.
77. Pedra CAC, Pedra SRF, Chaccur P, et al. Periventricular device closure of congenital muscular ventricular septal defects. *Expert Rev Cardiovasc Ther*. 2010;8:663–74.
78. Bendaly EA, Hoyer MH, Breinholt JP. Mid-term follow up of periventricular device closure of muscular ventricular septal defects. *Catheter Cardiovasc Interv*. 2011;78:577–82.
79. Geva A, McMahan CJ, Gauvreau K, Mohammed L, del Nido PJ, Geva T. Risk factors for reoperation after repair of discrete subaortic stenosis in children. *J Am Coll Cardiol*. 2007;50:1498–504.
80. Valeske K, Huber C, Mueller M, et al. The dilemma of subaortic stenosis—a single center experience of 15 years with a review of the literature. *Thorac Cardiovasc Surg*. 2011;59:293–7.
81. Miyamoto K, Nakatani S, Kanzaki H, Tagusari O, Kobayashi J. Detection of discrete subaortic stenosis by 3-dimensional transesophageal echocardiography. *Echocardiography*. 2005;22:783–4.
82. Maréchaux S, Juthier F, Banfi C, Vincentelli A, Prat A, Ennezat P-V. Illustration of the echocardiographic diagnosis of subaortic membrane stenosis in adults: surgical and live three-dimensional transesophageal findings. *Eur J Echocardiogr*. 2011;12:E2.
83. Hanna R, Chen MA, Gill EA. Cor triatriatum evaluated by real time 3D TEE. *Echocardiography*. 2011;28:E125–8.
84. Enar S, Singh P, Douglas C, et al. Live/real time three-dimensional transthoracic echocardiographic assessment of transposition of the great arteries in the adult. *Echocardiography*. 2009;26:1095–104.
85. Balzer J, Kühl H, Rassaf T, et al. Real-time transesophageal three-dimensional echocardiography for guidance of percutaneous cardiac interventions: first experience. *Clin Res Cardiol*. 2008;97:565–74.
86. Gripari P, Tamborini G, Barbier P, et al. Real-time three-dimensional transesophageal echocardiography: a new intraoperative feasible and useful technology in cardiac surgery. *Int J Cardiovasc Imaging*. 2010;26:651–60.
87. Scohy TV, Ten Cate FJ, Lecomte PVEL, et al. Usefulness of intraoperative real-time 3D transesophageal echocardiography in cardiac surgery. *J Card Surg*. 2008;23:784–6.
88. La Canna G, Arendar I, Maisano F, et al. Real-time three-dimensional transesophageal echocardiography for assessment of mitral valve functional anatomy in patients with prolapse-related regurgitation. *Am J Cardiol*. 2011;107:1365–74.
89. Swaans MJ, Van den Branden BJL, Van der Heyden JAS, et al. Three-dimensional transesophageal echocardiography in a patient undergoing percutaneous mitral valve repair using the edge-to-edge clip technique. *Eur J Echocardiogr*. 2009;10:982–3.
90. Brinkman V, Kalbfleisch S, Auseon A, Pu M. Real time three-dimensional transesophageal echocardiography-guided placement of left atrial appendage occlusion device. *Echocardiography*. 2009;26:855–8.
91. Perk G, Biner S, Kronzon I, et al. Catheter-based left atrial appendage occlusion procedure: role of echocardiography. *Eur Heart J Cardiovasc Imaging*. 2012;13:132–8.
92. Jánosi RA, Kahlert P, Plicht B, et al. Guidance of percutaneous transcatheter aortic valve implantation by real-time three-dimensional transesophageal echocardiography—A single-center experience. *Minim Invasive Ther Allied Technol*. 2009;18:142–8.
93. Horton KD, Whisenant B, Horton S. Percutaneous closure of a mitral perivalvular leak using three dimensional real time and color flow imaging. *J Am Soc Echocardiogr*. 2010;23:903.e5–7.
94. Jenkins C, Bricknell K, Chan J, Hanekom L, Marwick TH. Comparison of two- and three-dimensional echocardiography with sequential magnetic resonance imaging for evaluating left ventricular volume and ejection fraction over time in patients with healed myocardial infarction. *Am J Cardiol*. 2007;99:300–6.
95. Mor-Avi V, Jenkins C, Köhl HP, et al. Real-time 3-dimensional echocardiographic quantification of left ventricular volumes: multicenter study for validation with magnetic resonance imaging and investigation of sources of error. *JACC Cardiovasc Imaging*. 2008;1:413–23.
96. Sugeng L, Mor-Avi V, Weinert L, et al. Quantitative assessment of left ventricular size and function: side-by-side comparison of real-time three-dimensional echocardiography and computed tomography with magnetic resonance reference. *Circulation*. 2006;114:654–61.
97. Leibundgut G, Rohner A, Grize L, et al. Dynamic assessment of right ventricular volumes and function by real-time three-dimensional echocardiography: a comparison study with magnetic resonance imaging in 100 adult patients. *J Am Soc Echocardiogr*. 2010;23:116–26.
98. Sugeng L, Mor-Avi V, Weinert L, et al. Multimodality comparison of quantitative volumetric analysis of the right ventricle. *JACC Cardiovasc Imaging*. 2010;3:10–8.
99. Tamborini G, Marsan NA, Gripari P, et al. Reference values for right ventricular volumes and ejection fraction with real-time three-dimensional echocardiography: evaluation in a large series of normal subjects. *J Am Soc Echocardiogr*. 2010;23:109–15.
100. Shimada YJ, Shiota M, Siegel RJ, Shiota T. Accuracy of right ventricular volumes and function determined by three-dimensional echocardiography in comparison with magnetic resonance imaging: a meta-analysis study. *J Am Soc Echocardiogr*. 2010;23:943–53.
101. Fusini L, Tamborini G, Gripari P, et al. Feasibility of intraoperative three-dimensional transesophageal echocardiography in the evaluation of right ventricular volumes and function in patients undergoing cardiac surgery. *J Am Soc Echocardiogr*. 2011;24:868–77.
102. Karhausen J, Dudaryk R, Phillips-Bute B, et al. Three-dimensional transesophageal echocardiography for perioperative right ventricular assessment. *Ann Thorac Surg*. 2012;94:468–74.
103. Lang RM, Bierig M, Devereux RB, et al. Recommendations for chamber quantification. *Eur J Echocardiogr*. 2006;7:79–108.
104. Kapetanakis S, Kearney MT, Siva A, Gall N, Cooklin M, Monaghan MJ. Real-time three-dimensional echocardiography: a novel technique to quantify global left ventricular mechanical dyssynchrony. *Circulation*. 2005;112:992–1000.
105. Gorcsan III J, Abraham T, Agler DA, et al. Echocardiography for cardiac resynchronization therapy: recommendations for performance and reporting—a report from the American Society of Echocardiography Dyssynchrony Writing Group endorsed by the Heart Rhythm Society. *J Am Soc Echocardiogr*. 2008;21:191–213.
106. Tanaka H, Hara H, Adelstein EC, Schwartzman D, Saba S, Gorcsan J. Comparative mechanical activation mapping of RV pacing to LBBB by 2D and 3D speckle tracking and association with response to resynchronization therapy. *JACC Cardiovasc Imaging*. 2010;3:461–71.
107. Soliman OII, Geleijnse ML, Theuns DAMJ, et al. Usefulness of left ventricular systolic dyssynchrony by real-time three-dimensional echocardiography to predict long-term response to cardiac resynchronization therapy. *Am J Cardiol*. 2009;103:1586–91.
108. Kapetanakis S, Bhan A, Murgatroyd F, et al. Real-time 3D echo in patient selection for cardiac resynchronization therapy. *JACC Cardiovasc Imaging*. 2011;4:16–26.
109. Kleijn SA, Aly MF, Knol DL, et al. A meta-analysis of left ventricular dyssynchrony assessment and prediction of response to

- cardiac resynchronization therapy by three-dimensional echocardiography. *Eur Heart J Cardiovasc Imaging*. 2012;13:763–75.
110. Wang H, Shuraih M, Ahmad M. Real time three-dimensional echocardiography in assessment of left ventricular dyssynchrony and cardiac resynchronization therapy. *Echocardiography*. 2012; 29:192–9.
111. Seo Y, Ishizu T, Enomoto Y, et al. Validation of 3-dimensional speckle tracking imaging to quantify regional myocardial deformation. *Circ Cardiovasc Imaging*. 2009;2:451–9.
112. Ashraf M, Myronenko A, Nguyen T, et al. Defining left ventricular apex-to-base twist mechanics computed from high-resolution 3D echocardiography: validation against sonomicrometry. *JACC Cardiovasc Imaging*. 2010;3:227–34.
113. Andrade J, Cortez LD, Campos O, et al. Left ventricular twist: comparison between two- and three-dimensional speckle-tracking echocardiography in healthy volunteers. *Eur J Echocardiogr*. 2011;12:76–9.
114. Kleijn SA, Aly MFA, Terwee CB, van Rossum AC, Kamp O. Three-dimensional speckle tracking echocardiography for automatic assessment of global and regional left ventricular function based on area strain. *J Am Soc Echocardiogr*. 2011;24:314–21.
115. Kahlert P, Plicht B, Schenk IM, Janosi R-A, Erbel R, Buck T. Direct assessment of size and shape of noncircular vena contracta area in functional versus organic mitral regurgitation using real-time three-dimensional echocardiography. *J Am Soc Echocardiogr*. 2008;21:912–21.
116. Pérez de Isla L, Casanova C, Almería C, et al. Which method should be the reference method to evaluate the severity of rheumatic mitral stenosis? Gorlin's method versus 3D-echo. *Eur J Echocardiogr*. 2007;8:470–3.
117. Altioek E, Hamada S, van Hall S, et al. Comparison of direct planimetry of mitral valve regurgitation orifice area by three-dimensional transesophageal echocardiography to effective regurgitant orifice area obtained by proximal flow convergence method and vena contracta area determined by color Doppler echocardiography. *Am J Cardiol*. 2011;107:452–8.
118. Tsang W, Weinert L, Sugeng L, et al. The value of three-dimensional echocardiography derived mitral valve parametric maps and the role of experience in the diagnosis of pathology. *J Am Soc Echocardiogr*. 2011;24:860–7.
119. Veronesi F, Caiani EG, Sugeng L, et al. Effect of mitral valve repair on mitral-aortic coupling: a real-time three-dimensional transesophageal echocardiography study. *J Am Soc Echocardiogr*. 2012;25:524–31.
120. Badano LP, Muraru D. Towards an integrated echocardiographic assessment of valvular mechanics by three-dimensional volumetric imaging. *J Am Soc Echocardiogr*. 2012;25:532–4.
121. Lu X, Xie M, Tomberlin D, et al. How accurately, reproducibly, and efficiently can we measure left ventricular indices using M-mode, 2-dimensional, and 3-dimensional echocardiography in children? *Am Heart J*. 2008;155:946–53.
122. Riehle TJ, Mahle WT, Parks WJ, Sallee D, Fyfe DA. Real-time three-dimensional echocardiographic acquisition and quantification of left ventricular indices in children and young adults with congenital heart disease: comparison with magnetic resonance imaging. *J Am Soc Echocardiogr*. 2008;21:78–83.
123. Raedle-Hurst TM, Mueller M, Rentzsch A, Schaeffers H-J, Herrmann E, Abdul-Khalik H. Assessment of left ventricular dyssynchrony and function using real-time 3-dimensional echocardiography in patients with congenital right heart disease. *Am Heart J*. 2009;157:791–8.
124. Friedberg MK, Su X, Tworetzky W, Soriano BD, Powell AJ, Marx GR. Validation of 3D echocardiographic assessment of left ventricular volumes, mass, and ejection fraction in neonates and infants with congenital heart disease: a comparison study with cardiac MRI. *Circ Cardiovasc Imaging*. 2010;3:735–42.
125. Hascoët S, Briere G, Caudron G, Cardin C, Bongard V, Acar P. Assessment of left ventricular volumes and function by real time three-dimensional echocardiography in a pediatric population: a TomTec versus QLAB comparison. *Echocardiography*. 2010;27: 1263–73.
126. Laser KT, Bunge M, Hauße P, et al. Left ventricular volumetry in healthy children and adolescents: comparison of two different real-time three-dimensional matrix transducers with cardiovascular magnetic resonance. *Eur J Echocardiogr*. 2010;11:138–48.
127. Iriart X, Montaudon M, Lafitte S, et al. Right ventricle three-dimensional echocardiography in corrected tetralogy of fallot: accuracy and variability. *Eur J Echocardiogr*. 2009;10:784–92.
128. Khoo NS, Young A, Occleshaw C, Cowan B, Zeng ISL, Gentles TL. Assessments of right ventricular volume and function using three-dimensional echocardiography in older children and adults with congenital heart disease: comparison with cardiac magnetic resonance imaging. *J Am Soc Echocardiogr*. 2009;22: 1279–88.
129. van der Zwaan HB, Helbing WA, McGhie JS, et al. Clinical value of real-time three-dimensional echocardiography for right ventricular quantification in congenital heart disease: validation with cardiac magnetic resonance imaging. *J Am Soc Echocardiogr*. 2010;23:134–40.
130. Soriano BD, Hoch M, Ithuralde A, et al. Matrix-array 3-dimensional echocardiographic assessment of volumes, mass, and ejection fraction in young pediatric patients with a functional single ventricle: a comparison study with cardiac magnetic resonance. *Circulation*. 2008;117:1842–8.
131. Kutty S, Graney BA, Khoo NS, et al. Serial assessment of right ventricular volume and function in surgically palliated hypoplastic left heart syndrome using real-time transthoracic three-dimensional echocardiography. *J Am Soc Echocardiogr*. 2012;25: 682–9.
132. Hlavacek A, Lucas J, Baker H, Chessa K, Shirali G. Feasibility and utility of three-dimensional color flow echocardiography of the aortic arch: the “echocardiographic angiogram”. *Echocardiography*. 2006;23:860–4.
133. Pemberton J, Ge S, Thiele K, Jerosch-Herold M, Sahn DJ. Real-time three-dimensional color Doppler echocardiography overcomes the inaccuracies of spectral Doppler for stroke volume calculation. *J Am Soc Echocardiogr*. 2006;19:1403–10.
134. Poh KK, Levine RA, Solis J, et al. Assessing aortic valve area in aortic stenosis by continuity equation: a novel approach using real-time three-dimensional echocardiography. *Eur Heart J*. 2008; 29:2526–35.
135. Lu X, Nadvoretzkiy V, Klas B, et al. Measurement of volumetric flow by real-time 3-dimensional doppler echocardiography in children. *J Am Soc Echocardiogr*. 2007;20:915–20.
136. Rajpoot K, Grau V, Noble JA, Szmigielski C, Becher H. Multiview fusion 3-D echocardiography: improving the information and quality of real-time 3-D echocardiography. *Ultrasound Med Biol*. 2011;37:1056–72.